Linear viscoelastic dynamic wing torsional divergence and column creep buckling including failure probabilities and survival times

(Received: December 13, 2011. Revised: June 13, 2013. Accepted: June 16, 2013)

Harry H. Hilton[1]

Abstract

In this paper results of various analyses establish the following:

- The mathematical and physical similarities and differences between linear viscoelastic torsional divergence and column creep buckling are determined. In each case instabilities take place under constant loads at critical times.
- The existence of a material dependent load threshold below which only stable configurations are possible.
- Under static loads when the time dependence of the motion is solely material property dependent, the inclusion of inertia terms in the governing relations radically alters the type of motion and instability occurrences.
- Separate analyses based on material property considerations lead to failures and failure times distinct from those associated with torsional and buckling instabilities. Viscoelastic materials exhibit degradations of relaxation moduli and failure stresses with time. Consequently, since applied moments and deflections increase in time due to creep and failure stresses decrease, it is only a matter of time before either creep buckling or material failures will occur.

1. Introduction

The linear viscoelastic problems of column buckling and of lifting surface torsional divergence are strikingly similar from mathematical, physical and conceptual points of view and are analyzed in tandem. Considerably more literature is available on either elastic and viscoelastic column buckling than there is on its counterpart of torsional divergence. Consequently, columns will be primarily treated here and divergence will be analyzed by analogy.

In the elastic static buckling and torsional divergence cases, instability is indicated by proper interpretations of eigenvalues. Viscoelastic phenomena are inherently time dependent and one must seek critical times where instabilities begin to manifest themselves. A through understanding of elastic phenomena and their impact on viscoelastic action is necessary. Such an abbreviated treatment maybe found in Section 2.1.

In this paper, dynamic loading conditions and responses are formulated and investigated to determine their influences on creep buckling/torsional instability conditions of linear viscoelastic column/wing deterministic or probabilistic survival times. It also shown that viscoelastic static or dynamic column creep buckling and torsional divergence analyses are subject to additional load constraints, indicating that there is a threshold below which columns and wings will remain stable indefinitely, unless material failures take place.

It must, of course, be remembered that the present analysis is specific to linear small deformation viscoelastic columns and/or lifting surfaces. Although only structural columns and wings are considered here, it is important to note that opposite to elastic materials on the viscoelastic energy spectrum are viscous

[1] Professor Emeritus of Aerospace Engineering, h-hilton@illinois.edu, Aerospace Engineering Department & Private Sector Division of the National Center for Supercomputing Applications, University of Illinois at Urbana-Champaign (UIUC), 104 South Wright Street, 316 Talbot Lab., Urbana, IL 61801-2935 USA

doi:10.3293/asdj.2013.16

Table 1: Role of lateral disturbance force ΔF

Column	Modulus	Apply ΔF
Elastic, static [25]	Young's	Any order
Plastic, static [104]	Tangent	After P
Plastic, static [92]	Secant	Before P
Viscoelastic, static [33], [73]	Relaxation	Never
Elastic, dynamic [60], [61]	Young's	Before P
Viscoelastic, dynamic current paper	Relaxation	Never

fluids where in Refs. [14] and [15] the nonlinear creep buckling of fluid columns and jets have been investigated.

Other nonlinear contributions due to large deformations, material properties and/or follower loads [8], [44], [45], [50], [66], [102], [103], [112], are not treated here in order to isolate the influence of material properties and inertia contributions. Nor are structural control considerations included in the analysis, which would further delay creep instabilities[1] and/or material failures. See [3], [4], [47], and [111].

2. Analysis

2.1 Elastic, plastic and viscoelastic stability criteria

Static elastic column buckling theory is well established based on the [25] formulation. Euler's model postulates a centrally loaded, perfectly straight, homogeneous, isotropic, linear elastic column. Under these stipulated conditions it is necessary to apply and remove infinitesimal lateral disturbances in order to investigate the stability of the bent column forms, which occur at eigenvalues of the applied load, i.e., the Euler loads. Since elastic materials are conservative the order, manner and duration of static load applications do not influence these eigenvalues. In non-conservative material systems with plastic behavior, however, the lateral disturbance application sequence is of paramount importance as it leads to either reduced modulus [92] or tangent modulus [24], [104] theories depending on the order of application of the lateral disturbance and the axial compressive load. (See Table 1.) The texts [1], [2], [10], [20], [26], [29], [65], [66], [71], [72] and [95] among others, contain detailed expositions of elastic and inelastic buckling. Ref. [23] treats deterministic and stochastic stability of elastic columns, plates and shells, while in [30] Lyapunov dynamic stability criteria for plates are examined.

Extensive data bases of viscoelastic properties for distinct materials may be found in [64], [69] and [81] which clearly show the dissipative nature of all viscoelastic materials. Additionally, viscoelastic column deflections are a series of successive stable bent forms in time until either creep buckling or material failure takes place. Since the material is non-conservative through its inherent time dependent energy dissipation, the elastic Euler model of lateral disturbance applications is neither applicable nor permissible. Continuous bending in time

[1]The generic terms stability/instability refer to columns or lifting surfaces or both.

must, therefore, be achieved through modeling of real column conditions, such as eccentric loads or the inclusion of initial imperfections or both.

Classical elastic and viscoelastic analytical buckling and torsional divergence instability definitions are expressed by

$$\text{instability conditions}\begin{cases}\text{elastic}\begin{cases}\text{column} \implies \lim\limits_{P\to P_E}\left[w^e(P) \quad \text{or} \quad \dfrac{\partial w^e(P)}{\partial P}\right] \to \infty \\ \text{buckling} \\ \text{torsional} \implies \lim\limits_{V\to V_D^e}\left[\theta^e(V) \quad \text{or} \quad \dfrac{\partial \theta^e(V)}{\partial V}\right] \to \infty \\ \text{divergence}\end{cases} \\ \text{viscoelastic}\begin{cases}\text{creep} \implies \lim\limits_{t\to t_{cr}^B}\left[w(t) \quad \text{or} \quad \dfrac{\partial w(t)}{\partial t}\right] \to \infty \\ \text{buckling} \qquad (P<P_E) \\ \text{torsional} \implies \lim\limits_{t\to t_{cr}^D}\left[\theta(t) \quad \text{or} \quad \dfrac{\partial \theta(t)}{\partial t}\right] \to \infty \\ \text{divergence} \qquad (V<V_D^e)\end{cases}\end{cases} \tag{1}$$

with the Euler load $P_E = \mathcal{C}\pi^2 E_0/L^2$ and where the end fixity coefficient $\mathcal{C}$ values are dictated by the column boundary conditions.

In Refs. [33], [37], [73] and [67] it is shown that for quasi-static linear viscoelastic columns no finite critical times t_{cr} exist for $0 < P < P_E$, where P_E is the Euler load for an equivalent elastic column. However, experimental evidence indicates that real viscoelastic columns buckle at a finite time [2], [29], [31], [63]. In the absence of analytical results indicating $t_{cr} < \infty$ for linear viscoelastic columns, finite ultimate times have been formulated in [33] based on time dependent material failure conditions prescribed by the [91] interaction curves. Subsequently, in [44] and [46] probabilistic delamination buckling failures have been analyzed based on the more general [43] invariant failure surface criterion in order to establish survival times based on viscoelastic material failures rather than stability considerations. A different criterion based on finite creep strains has also been proposed in [28]. Additionally, even nonlinear viscoelastic column models do not necessarily achieve finite t_{cr} times as defined by Eqs. (1) under some circumstances [35]. Torsional creep divergence problems of viscoelastic lifting surfaces obey the same phenomenological and mathematical principles as does creep buckling of viscoelastic columns [34], [36], [49]. In particular, it has been demonstrated that the inclusion of inertia terms, at either small or large relaxation times, in the torsional governing equations significantly alters both deflection responses and stability considerations. In [59], [60] and [61] extensive analyses of dynamic effects on elastic column buckling has been presented and it is concluded that their effects are indeed significant. Vibration of elastic columns under time dependent loads with static Euler instability has been investigated in [11] and [12].

Viscoelastic quasi-static creep buckling of more complex systems, such as composites, have been studied in [107] (laminated columns), [108] (laminated plates), [46] (static stochastic column delaminations), [5] piezoelectric column control) and [45] (follower loads). Stochastic conditions manifest themselves due to the uncertainties of constitutive relations [39] (geometries, temperatures[2] applied loads and failure conditions [43], [84], [85], [105].

[2]For a bibliography of random temperature effects on structures and materials, see [39].

Table 2: Column and wing coordinates

Item	x_1 -direction	x_2-direction	x_3-direction
column	longitudinal	neutral axis (NA)	normal to NA
wing	span	chord at zero angle of attack	normal to chord at zero angle of attack

Elastic torsional divergence is extensively treated in Refs. [9], [21], [22], [57], [89], and [109]. The governing ODEs in time are identical, except for coefficient values, to the governing column ODEs and consequently result in similar eigenvalue stability considerations. One minor exception is the usual presence of a built-in rigid body of attack which removes the necessity of the equivalent ΔF torque to initiate torsional deflections.

The aero-viscoelasticity literature is considerably more sparse, however [54], [55], [78], [79] and [80] carry a considerable number of references. The quasi-static torsional divergence problem was first formulated in [36].

2.2 Generalized viscoelastic formulations

In a Cartesian coordinate system, $x = \{x_i\}$ with $i = 1, 2, 3$, consider a linear, isothermal, homogeneous and prismatic wing or column of length L and with an initial imperfection $\theta_0(x_1)$ and $w_0(x_1)$ respectively and defined by the truncated series when $R < \infty$ and by a Fourier series for $R = \infty$.

$$\left\{ \begin{array}{c} \theta_0(x_1) \\ \\ w_0(x_1) \end{array} \right\} = \sum_{r=1}^{R} \left\{ \begin{array}{c} \theta_r^0 \\ \\ w_r^o \end{array} \right\} \sin\left(\frac{r\,\pi\,x_1}{L}\right) \qquad 1 \le R \le \infty \tag{2}$$

The coordinate systems are defined in Table 2. The 1–D homogeneous viscoelastic isothermal constitutive relations are given by

$$\sigma_{11}(x_1,t) \;=\; E_0 \int_{-\infty}^{t} E(t-t')\,\frac{\partial \epsilon_{11}(x_1,t')}{\partial t'}\,dt' \;=\; E_0 \int_{-\infty}^{t} E^*(t-t')\,\epsilon_{11}(x_1,t')\,dt' \tag{3}$$

and

$$\epsilon_{11}(x_1,t) \;=\; C_0 \int_{-\infty}^{t} C(t-t')\,\frac{\partial \sigma_{11}(x_1,t')}{\partial t'}\,dt' \;=\; C_0 \int_{-\infty}^{t} C^*(t-t')\,\sigma_{11}(x_1,t')\,dt' \tag{4}$$

where $E^*(t) = \dfrac{\partial E(t)}{\partial t}$, $C^*(t) = \dfrac{\partial C(t)}{\partial t}$, with E_0 and C_0 are respectively the initial elastic modulus and compliance, $E(t)$ the relaxation modulus and $C(t)$ the creep compliance. The latter are related to each other through their Fourier transforms (FT) by

$$\overline{\overline{E^*}}(\omega) \;=\; \frac{1}{\overline{\overline{C^*}}(\omega)} \;=\; \imath\,\omega\,\overline{\overline{E}}(\omega) \;=\; \frac{1}{\imath\,\omega\,\overline{\overline{C}}(\omega)} \tag{5}$$

For viscoelastic materials with initial elastic conditions (ICs) $\epsilon_{ij}(x,0) = \epsilon_{ij}^E(x,0)$, there are two classes depending on the presence of E_∞, the fully relaxed modulus. The normalized relaxation modulus w.r.t. E_0 is defined by Prony series as [87]

$$E(t) \;=\; \begin{cases} \textbf{Class I materials}: \\ \displaystyle\sum_{n=1}^{N} E_n \;\exp\left(-\frac{t}{\tau_n}\right), \qquad \lim_{t\to\infty}\;\epsilon(t)=\infty, \quad \displaystyle\sum_{n=1}^{N} E_n \;=\; 1, \\ \qquad\qquad\qquad\qquad\qquad\qquad\qquad\qquad\qquad\qquad E_\infty \;=\; 0 \\ \\ \textbf{Class II materials}: \\ E_\infty + \displaystyle\sum_{n=1}^{N} E_n \;\exp\left(-\frac{t}{\tau_n}\right), \quad \lim_{t\to\infty}\;\epsilon(t)<\infty, \quad E_\infty + \displaystyle\sum_{n=1}^{N} E_n = 1 \end{cases} \tag{6}$$

and where $E_n,\; E_\infty, \tau_n$ and $N \le \infty$ are viscoelastic material property parameters and $E_0$is the instantaneous (elastic) modulus.

The four possible classes of viscoelastic behavior based on initial and long time responses are shown Table 3. Classes III and IV describe fluid behavior with $\epsilon^E(x,0)=0$ and do not apply to the present column or divergence problem formulations (See Table 3).

The governing relations for isothermal isotropic homogeneous prismatic configurations are

$$\text{column creep buckling } (P \text{ or } P(t) \;<P_E) \implies$$

$$\underbrace{m\,\frac{\partial^2 w(x_1,t)}{\partial t^2}}_{\substack{\text{inertia force}\\ (\mathrm{T}_{1\mathrm{w}})}} \;+\; \underbrace{I\int_{-\infty}^{t} E(t-t')\frac{\partial^5 w(x_1,t')}{\partial x_1^4\,\partial t'}\,dt'}_{\substack{\text{load due to viscoelastic}\\ \text{internal bending moment } (\mathrm{T}_{2\mathrm{w}})}} \;=$$

$$\underbrace{P(t)\frac{\partial^2}{\partial x_1^2}\left[w(x_1,t) - \overbrace{w_0(x_1)}^{\substack{\text{initial}\\ \text{imperfection}}}\right]}_{\substack{\text{load due to applied}\\ \text{external bending moment } (\mathrm{T}_{3\mathrm{w}})}} \tag{7a}$$

$$\text{lifting surface creep torsional divergence } (V \text{ or } V(t) < V_D^e) \implies$$

$$\underbrace{I_P\frac{\partial^2\theta(x_1,t)}{\partial t^2}}_{\substack{\text{rotational}\\ \text{inertia } (\mathrm{T}_{1\theta})}} \;+\; \underbrace{J\int_{-\infty}^{t} G(t-t')\frac{\partial^3\theta(x_1,t')}{\partial x_1^2\,\partial t'}\,dt'}_{\text{torsional rigidity } (\mathrm{T}_{2\theta})} \;=$$

$$\underbrace{\frac{\rho\,C_\ell\,c^2\,V(t)^2}{2}\left[\underbrace{\theta(x_1,t)}_{\substack{\text{flexible body}\\ \text{contribution}}} \;\underbrace{-\overbrace{\theta_0(x_1)}^{\substack{\text{initial}\\ \text{twist}}} - \overbrace{\alpha_0(x_1)}^{\substack{\text{angle}\\ \text{of zero}\\ \text{lift}}} + \overbrace{\alpha_r(x_1,t)}^{\substack{\text{trim}\\ \text{angle}}}}_{\substack{=\,\theta_r(x_1,t)\\ \text{rigid body contribution}}}\right]}_{\text{applied aerodynamic torque } (\mathrm{T}_{3\theta})} \tag{7b}$$

with solutions

$$w(x_1,t) \;=\; \sum_{n=1}^{R_w} W_n(t)\; f_{nw}(x_1) \qquad 1 \le n \le R_w \le \infty \tag{8a}$$

$$\theta(x_1,t) \;=\; \sum_{n=1}^{R_w} \Theta_n(t)\; f_{n\theta}(x_1) \qquad 1 \le n \le R_w \le \infty \tag{8b}$$

Table 3: Classification of viscoelastic behavior

Class	Initial Strain	Long Time Strain	Moduli	Material Type
I	$\epsilon^E(x,0)$	∞	$E_0 > 0, E_\infty = 0$	solids
II	$\epsilon^E(x,0)$	$< \infty$	$E_0 > 0, E_\infty > 0$	solids
III	0	∞	$E_0 = 0, E_\infty = 0$	fluids
IV	0	$< \infty$	$E_0 = 0, E_\infty > 0$	fluids

Note that the initial imperfection twist angle $\theta_0(x_1)$, unlike the initial column imperfection $w(x_1)$, may be zero provided either α_0 or α_r or both have non-zero values. The flight velocity V and trim angle α_r may vary with time due to maneuvers, buildups, landings/takeoffs, etc., as shown in [78]. Conceptually, this is equivalent to time dependent axial loads P on the column and in both cases leads to integral-partial-differential-equations (IPDEs) with time dependent (variable) coefficients. For equivalent elastic configurations, the time integrals and derivatives in terms T_2 are removed and PDEs result. Furthermore, in the legacy problems where inertia terms T_1 are neglected and for symmetric column BCs where spatial derivatives of order 2 are sufficient, Eqs. (7) are of the same order. Generally, except for the flag pole column, the BCs for columns will be distinct from those for the lifting surfaces. Such dissimilar conditions, however, do not negate the general similar behavior of buckling and torsional divergence phenomena.

The RHS of Eqs. (7) can be expressed in general terms as

$$\{\boldsymbol{F}(t)\} \;=\; \left\{ \begin{array}{c} P(t) < P_E \\ \\ \dfrac{\rho\, C_\ell\, c^2}{2}\,[V(t)]^2\,, \quad V(t) < V_D^e \end{array} \right\} \tag{9}$$

Substitution of Eqs. (8) into the governing relations (7) or the application of Galerkin's method to the latter, reduces these two equations in both cases to time domain universal linear governing relations of the form

$$\boldsymbol{A}_{mn2}\frac{\partial^2 \boldsymbol{u}_{mn}(t)}{\partial t^2} \;+\; \boldsymbol{A}_{mn1}\int_{-\infty}^{t} \boldsymbol{D}(t-t')\frac{\partial \boldsymbol{u}_{mn}(t')}{\partial t'}\,dt' \;+\; \boldsymbol{A}_{mn0}\,\boldsymbol{F}(t)\;\boldsymbol{u}_{mn}(t) \;=$$

$$\boldsymbol{A}_{mn00}\;\boldsymbol{F}(t) \qquad 1 \le m \le 2 \qquad \text{and} \qquad 1 \le n \le R_w \le \infty \tag{10}$$

with

$$\boldsymbol{D}(t) \;=\; \left\{ \begin{array}{c} E(t) \\ \\ G(t) \end{array} \right\} \qquad \text{and} \qquad \left\{ \begin{array}{c} \boldsymbol{u_{1n}}(t) \\ \\ \boldsymbol{u_{2n}}(t) \end{array} \right\} \;=\; \left\{ \begin{array}{c} W_n(t) \\ \\ \Theta_n(t) \end{array} \right\}$$

$$1 \le n \le R_w \le \infty \tag{11}$$

and where the $\boldsymbol{A_{nj}}$ may have distinct values depending on which of the two computational methods for removing the spatial dependence are used. Both the column and the torsional divergence phenomenon are closed loop systems subject to instabilities based on either the axial critical load $P(t)$ or the velocity $V(t)$. The stability criteria are displayed in Eqs. (1).

For simulations to be truly physically representative of real elastic or viscoelastic columns, the load $P(t)$ cannot be imposed "instantaneously" within

Table 4: List of characteristic times

Time	Definition	Eq.	Criterion	Fig.
t_0	time at which relaxation begins $t_0 \approx 10^{-3}$	(1)	$E(t) = E_0$ for $0 \le t \le t_0$	3
t_1	time when load stabilizes at its maximum P_0, $t_1 \approx 10^{-4}$	(12)	$P(t) \le P_0$ for $0 \le t \le t_1$	1
t_R	time to reach fully relaxed modulus E_∞, $t_R \approx 10$	(3)	$E(t) = E_\infty$	3
t_2	time for sound wave to travel length of column to $x = L, t_2 \approx 10^{-2}$		$t_L = L/c_0$ for $t \ge t_R$	

the present dynamic time frame, since the loading sequence significantly influences dynamic displacement responses particularly in early times. Moreover, $P(t)$ must be modeled with the following conditions in mind. In order to properly reflect initial ($t < t_0$) elastic column equivalences (Figs. 1, 10 - 22), the time t_1 needed to stabilize $P(t)$ must be shorter than the time $t_0 > 0$ when relaxation begins. Therefore, the following conditions must be imposed on $P(t)$ during the loading cycle to model physical loading realities [8]

$$P(t) = \begin{cases} P_0 \; F_P(t) & 0 \le t \le t_1 \\ P_0 & t \ge t_1 \end{cases} \tag{12}$$

with

$$F_P(0) = 0, \quad F_P(t_1) = 1, \quad \frac{dF_P(0)}{dt} = \frac{dF_P(t_1)}{dt} = 0 \tag{13}$$

Some possible forms of the loading function $F_P(t)$ are (See Fig. 1 with $k = 2$ and $l = 4$)

$$F_P(t) = \left\{ \begin{array}{ll} A_k \left(\frac{t}{t_1}\right)^k + A_l \left(\frac{t}{t_1}\right)^l \quad k,l \ge 2 & \text{Load A} \\ \frac{1}{2}\left[1 - \cos\left(\frac{\pi\, t}{t_1}\right)\right] & \text{Load B} \\ H(t) & \text{Load C} \\ \frac{t}{t_1} & \text{Load D} \end{array} \right\}$$

$$0 \le t \le t_1 < t_0 \tag{14}$$

where the exponents k and l need not necessarily be integers. Other similar loading patterns can be readily constructed. Load C, while mathematically attractive, is physically unattainable as it fails to meet the conditions of Eqs. (13). Load D has some characteristics of achieving an acceptable loading time ramp rise, but does not satisfy the zero slope requirements of Eqs. (13). Representative time values related to loading patterns and relaxation functions are displayed in Table 4. Similar functions can be generated for the flight velocities $V(t)$ as demonstrated in [78].

A solution corresponding to the initial imperfection of Eq. (2) is given by

$$w(x_1, t) = \sum_{r=1}^{R} W_r(t) \; \sin\left(\frac{r\,\pi\, x_1}{L}\right) \tag{15}$$

From Eq. (7a) one then obtains the governing relations for each amplitude $W_r(t)$ as

$$\ddot{W}_r(t) \;+\; \lambda_r^4 \int_{-\infty}^{t} E(t-t')\,\dot{W}_r(t')\;dt' \;-\; D_r^{lf}(t)\left[W_r(t)-w_r^0\right] \;=\; 0$$

$$r = 1, 2, 3, \cdots, R \tag{16}$$

with $P = P(t)$ defined by Eq. (12), and with

$$\lambda_r^4 \;=\; \frac{E_0\, I}{\rho}\left(\frac{r\,\pi}{L}\right)^4 \;=\; r^2\, P_r^* \tag{17}$$

$$D_r^{lf}(t) \;=\; \begin{cases} e\, P_r^*\, F_P(t) & 0 \le t \le t_1 \\ e\, P_r^* & t \ge t_1 \end{cases} \tag{18}$$

where

$$P_r^* \;=\; \frac{P_E}{\rho}\left(\frac{r\,\pi}{L}\right)^2 \quad \text{and} \quad P_E \;=\; \frac{E_0\, I\, \pi^2}{L^2} \quad \text{with} \quad P_0 \;=\; e\, P_E \quad 0 < e < 1 \tag{19}$$

With the $D_r^{lf}(t)$ loading function present in Eq. (16) the integral–differential relation cannot be solved by integral transforms and must be solved directly in the time space. However, a Laplace transform (LT) can be applied to Eq. (16) with $D_r^{lf}(t) \approx D_{r\infty}^{lf}$, or more precisely $\lim\limits_{t\to\infty} D_r^{lf}(t) \to D_{r\infty}^{lf}$, in order to estimate long time behavior, which results in

$$\text{dynamic viscoelastic} \;\Longrightarrow\; \overline{W}_r(p) \;=\; \frac{\lambda_r^4\, \overline{E}(p)\, w_r^o}{p\left[p^2 + \lambda_r^4\, \overline{E}(p) - D_{r\infty}^{lf}\right]} \tag{20}$$

where $\overline{F}(p) = \int\limits_0^{\infty} \exp(-p\;t)\;F(t)\;dt$ is the LT of $F(t)$. As seen in Appendix A these results are exact for Load C of Eqs. (14).

Similarly, the LT of the dynamic elastic solution becomes

$$\text{dynamic elastic} \;\Longrightarrow\; \overline{W}_r^{e}(p) \;=\; \frac{\lambda_r^4\, w_r^o}{p\left[p^2 + \lambda_r^4 - D_{r\infty}^{lf}\right]} \tag{21}$$

whereas the corresponding quasi-static solution transforms are given by

$$\text{quasi}-\text{static viscoelastic} \;\Longrightarrow\; \overline{W}_r^{qs}(p) \;=\; \frac{\lambda_r^4\, \overline{E}(p)\, w_r^o}{p\left[\lambda_r^4\, \overline{E}(p) - D_{r\infty}^{lf}\right]} \tag{22}$$

and

$$\text{quasi}-\text{static elastic} \;\Longrightarrow\; \overline{W}_r^{qse}(p) \;=\; \frac{\lambda_r^4\, w_r^o}{p\left[\lambda_r^4 - D_{r\infty}^{lf}\right]} \tag{23}$$

Stability estimates at $t = \infty$ may be realized through the application the LT limit theorem to Eqs. (20) and (22), such that for the quasi-static viscoelastic column response one obtains

$$\lim_{t\to\infty} W_r(t) \;=\; \lim_{p\to 0}\{p\,\overline{W}_r(p)\} \longrightarrow \frac{\lambda_r^4\, E_\infty\, w_r^o}{\lambda_r^4\, E_\infty - D_{r\infty}^{lf}} \;=\; \frac{w_r^o}{1 - \dfrac{e}{r^2\, E_\infty}} < \infty$$

$$\text{if} \quad r^2\, E_\infty \neq e < 1 \tag{24}$$

with

$$D_{r\infty}^{lf} \;=\; \lim_{t\to\infty} D_r^{lf}(t) \;=\; \lim_{p\to 0}\{p\,\overline{D}_r^{lf}(p)\} \;\longrightarrow\; e\, P_r^* \tag{25}$$

Note that $D_{r\infty}^{lf}$ is independent of the ramp loading function as it represents a long time ($t \gg t_1$) steady state load. An exact formulation of $D_r^{lf}(t)$ for the various loading functions of Eqs. (14) is given in Appendix A with the results represented by Eqs. (70).

The equivalent static or dynamic elastic solutions at $t \to \infty$ are

$$\lim_{t\to\infty} W_r^e(t) \;=\; \lim_{p\to 0}\{p\,\overline{W}_r^e(p)\} \longrightarrow \frac{\lambda_r^4\, w_r^o}{\lambda_r^4 - D_r^{lf}} \;=\; \frac{w_r^o}{1-\dfrac{e}{r^2}} < \infty \quad \text{if} \quad r^2 \neq e < 1 \tag{26}$$

It can be readily seen that the long time viscoelastic deflection is larger than the corresponding elastic one, due to

$$\frac{w_r^o}{1-\dfrac{D_r^{lf}}{\lambda_r^4}} \;<\; \frac{w_r^o}{1-\dfrac{D_r^{lf}}{\lambda_r^4\, E_\infty}} \quad \text{or} \quad \frac{w_r^o}{1-\dfrac{e}{r^2}} \;<\; \frac{w_r^o}{1-\dfrac{e}{r^2\, E_\infty}} \quad \text{since} \quad E_\infty < 1 \tag{27}$$

and that at $t \to \infty$ the pair of viscoelastic quasi-static and dynamic limits are equal to each other as is the corresponding elastic pair.

While the limit theorem is most useful in establishing values of functions at $t = 0$ or ∞, it offers no help in the temporal range $0 < t < \infty$. The fact that a function is bounded at both ends of its interval $[0, \infty]$, does not in any way guarantee its stability elsewhere in the region. Consider the simple example of the following LT function $\overline{f}(p)$ and its inverse $f(t)$.

$$f(t) \;=\; \frac{1}{t-a} \quad \text{and} \quad \overline{f}(p) \;=\; \lim_{B\to\infty}\{\exp(-ap)\,[Ei(ap - pB) - Ei(ap)]\} \tag{28}$$

with

$$\lim_{\substack{t\to 0\\ t\to\infty}} f(t) \;=\; \lim_{\substack{p\to\infty\\ p\to 0}} \left\{p\overline{f}(p)\right\} \;=\; 0 \tag{29}$$

where Ei is the exponential integral. The two limits of Eqs. (29) give no hint of the presence of a singularity at $t = a$.

The LT or Fourier transform (FT) inversions of Eqs. (20) to (23) for that interval involve such complicated functions that these inversions can only be evaluated numerically through fast Fourier transform (FFT) approaches [101] or analytically through Post's formula [86]

$$f(t) \;=\; \mathscr{L}^{-1}\left\{\overline{f}(s)\right\} \;=\; \lim_{k\to\infty} \frac{(-1)^k}{k!}\left(\frac{k}{t}\right)^{k+1} \frac{d^k\overline{f}(s)}{ds^k}\bigg|_{s=k/t} \tag{30}$$

The approximate inversion technique developed in [90] which has proved very useful and accurate in quasi-static problems when solutions are proportional to $\exp(-t/\tau)$, unfortunately does not enjoy the same success in dynamic problems where the solutions depend on $\exp(t/\tau)$.

Another approach is to solve Eqs. (7a) and (16) directly in the real time plane. A solution is in the form

$$W_r(t) \;=\; w_r\; e^{-\alpha_r\, t} \;+\; w_r^* \tag{31}$$

which from Eq. (16) then yields

$$\alpha_r^2 \;+\; \lambda_r^4\; e^{\alpha_r\, t} \int_{-\infty}^{t} E(t-t')\; e^{-\alpha_r\, t'}\; dt' \;-\; D_r^{lf}(t) \;=\; 0 \tag{32}$$

and

$$w_1^* \;=\; w_o \qquad b_0 \neq 0 \tag{33}$$

It is relatively easier to examine creep buckling criteria for the DE rather than integral constitutive relations. The governing relation Eq. (7) and (16) may also be stated in a differential form based on the constitutive relation

$$\mathcal{P}\{\sigma_{11}\} \;=\; E_0\,\mathcal{Q}\{\epsilon_{11}\} \tag{34}$$

with

$$\mathcal{P} \;=\; \sum_{n=0}^{s} a_n\,\frac{\partial^n}{\partial t^n} \qquad \text{and} \qquad \mathcal{Q} \;=\; \sum_{n=0}^{s} b_n\,\frac{\partial^n}{\partial t^n} \tag{35}$$

where $a_n,\ b_n\ (n = 0,\ 1,\ 2,\ \cdots,\ s)$ and s are material property parameters. The interdependence of the limits s and N of Eqs. (6) are derived in [38]. The differential form of the constitutive relations results in

$$\mathcal{P}\left\{\rho\,\frac{\partial^2 w(x_1,t)}{\partial t^2} \;+\; P(t)\,\frac{\partial^2 w(x_1,t)}{\partial x_1^2}\right\} + E_0\,I\,\mathcal{Q}\left\{\frac{\partial^4 w(x_1,t)}{\partial x_1^4} \;-\; \frac{d^4 w_o(x_1)}{dx_1^4}\right\} = 0 \tag{36}$$

and from Eq. (15), the amplitudes $W_r(t)$ are defined by

$$\mathcal{P}\left\{\ddot{W}_r(t) \;-\; D_r^{lf}(t)\,W_r(t)\right\} \;+\; \lambda_r^4\,\mathcal{Q}\{W_r(t) \;-\; w_r^o\} \;=\; 0 \tag{37}$$

It is readily seen from Eqs. (35) that the relationship (37) now reads

$$\underbrace{\frac{d^{s+2}W_r(t)}{dt^{s+2}} \;+\; a_{s-1}\frac{d^{s+1}W_r(t)}{dt^{s+1}}}_{\text{inertia terms}} \;+$$

$$\sum_{n=0}^{s}\left[\overbrace{\underbrace{\lambda_r^4\,b_n}_{\substack{\text{internal}\\ \text{bending}}} \;-\; \underbrace{D_r^{lf}(t)\,a_n}_{\substack{\text{applied}\\ \text{load}}} \;+\; \underbrace{a_{n-2}}_{\substack{\text{inertia}\\ \text{terms}}}}^{A_{nr}(t)}\right]\frac{d^n W_r(t)}{dt^n} \;=\; \overbrace{\underbrace{\lambda_r^4\,b_0\,w_r^o}_{\substack{\text{initial}\\ \text{imperfection}}}}^{B_{0r}} \tag{38}$$

where

$$a_s \;=\; 1, \quad A_{nr} \;=\; \left(r^2\,b_n - e\,a_n\right)P_r^* + a_{n-2}, \quad B_{0r} \;=\; r^2\,P_r^*\,b_0\,w_r^o$$
$$\text{with} \quad n-2 \geq 0 \qquad r = 1,2,3\cdots R \qquad \text{and} \qquad 0 \leq n \leq s \tag{39}$$

Note that an increasing deflection can only occur if

$$0 < \frac{b_0}{a_0} < e(t) = \frac{P(t)}{P_E} < 1$$
$$\text{since then at least for r} \;=\; 1, \quad A_{01} \;=\; (b_0 - e\,a_0)\,P_r^* < 0 \tag{40}$$

because all material property parameters a_n and b_n for $0 \leq n \leq s$ are non negative. Viscoelastic constitutive relations for materials with unbounded long time strains are characterized by $\mathcal{Q}$ operators of Eqs. (35) with $b_0 = 0$ [17], [38].

In general then, the following pattern emerges for additional viscoelastic column loading constraints ζ_{TH} which are the material dependent threshold values above which creep buckling is possible

Column creep buckling thresholds

Class I materials :

$$b_0 = 0,\ \lim_{t\to\infty}\{\epsilon_{ij}(t)\} \to \infty \Longrightarrow \quad \lim_{t\to t_{cr}}\{w(t)\} \to \infty \quad \text{for} \quad 0 < e(t) < 1$$
$$\text{with} \quad \zeta_{TH}(E_n,\tau_n,N) \;=\; 0$$

Class II materials :

$$b_0 \neq 0,\ \lim_{t\to\infty}\{\epsilon_{ij}(t)\} < \infty \Longrightarrow \quad \lim_{t\to t_{cr}}\{w(t)\} \to \infty \tag{41}$$
$$\text{for} \quad 0 < \zeta_{TH}(E_n,\tau_n,N) < e(t) < 1$$
$$e(t) \;=\; \frac{P(t)}{P_E}$$

Table 5: Critical creep buckling/divergence times

Time	Definition	Eq.	Criterion	Fig.
t_{cr}	$\lim_{t\to t_{cr}} \{w(x,t)\} \longrightarrow \infty$	(1)	classical creep buckling definition	8
t^{ϵ}_{cr}	$\lim_{t\to t^{\epsilon}_{cr}} \left\{ \frac{\partial \epsilon^T(x,t)}{\partial t} \right\} \longrightarrow 0$	(46)	compressive + bending strain reversal	23
t^{*}_{cr}	$\lim_{t\to t^{*}_{cr}} \left\{ \log \left[\frac{\partial w(x,t)}{\partial t} \right] \right\} \longrightarrow$ const.	(47)	constant log[deformation] rate	25
t_{LF}	$F_1(\sigma_{applied}, t_{LF}) \leq F_2(\sigma_{failure}, t_{LF})$ prescribed $\widetilde{P}(t_{LF}) \leq 1$	(55)	deterministic or stochastic material failure	27
t_{LFD}	prescribed design life time t_{LFD}		deterministic or stochastic material failure	

Note: If θ is substituted for w then Table 5 plies to torsional divergence

The functions $\zeta_{TH}(E_n, \tau_n, N)$ are prescribed by each material's constitutive relations (3) and must be determined on a case by case basis. For the differential constitutive relation representation of Eq. (38), the parameter ζ_{TH} is given by

$$\zeta_{TH}(E_n, \tau_n, N) \;=\; \zeta_{TH}(a_n, b_n, s) \;=\; \begin{cases} 0 & \text{Class I materials} \\ \dfrac{b_0}{a_0} & \text{Class II materials} \end{cases} \tag{42}$$

with each material possessing different values for the two material property coefficients a_0 and b_0.

Starting with Eq. (7b) and by repeating the same process, one can arrive a similar conditions for the creep divergence threshold.

Torsional creep divergence thresholds

Class I materials :
$b_0 = 0,\ G_\infty = 0,$
$\lim_{t\to\infty} \{\theta(t)\} \to \infty \Longrightarrow \quad \lim_{t\to t_{cr}} \{\theta(t)\} \to \infty \quad \text{for} \quad 0 < e^{\theta}(t) < 1$

$$\text{with} \quad \zeta^{\theta}_{TH}(G_n, \tau_n, N) \;=\; 0$$

Class II materials :
$b_0 \neq 0,\ G_\infty > 0,$
$\lim_{t\to\infty} \{\theta(t)\} < \infty \Longrightarrow \quad \lim_{t\to t_{cr}} \{\theta(t)\} \to \infty$

$$\text{for} \quad 0 < \zeta^{\theta}_{TH}(G_n, \tau_n, N) < e^{\theta}(t) < 1$$

$$e^{\theta}(t) \;=\; \frac{V(t)}{V^{e}_{D}} \tag{43}$$

2.3 Alternate definitions of creep buckling times

While column stability can be readily defined as a finite $w(x_1,t)$ at large times, the precise analytical pin-pointing of creep buckling instabilities at finite times is considerably more elusive. The classical formal definition of t_{cr} of Eq. (1) does not lead to finite time values as has been demonstrated in [33], [37] and [67] for static viscoelastic columns. It is shown in the present paper that the same holds true for dynamic columns as well. It is, therefore, necessary to prescribe and adopt other more realizable criteria based on auxiliary stability requirements or on material failure criteria. Table 5 summarizes the various definitions of creep buckling critical times. A similar table can be prepared for creep torsional divergence by substituting $\theta(t)$ for $w(t)$ and eliminating the strain reversal entry, which does not exists in shear.

The first three conditions in Table 5 are stability criteria while the last two are based on material and/or structural failures. It must, however, be realized that implicitly there corresponds a probability of failure to each of the five line items in Table 5.

2.3.1 Creep buckling definition based on strain reversal

The column is subjected to compressive strains $\epsilon_c(x_1,t)$ due to axial loads $P(t)$ and to bending strains $\epsilon_b(x_1,x_2,t)$ due to bending moments $P(t)w(x_1,t)$. The total strain is the sum of these two as given by

$$\epsilon_{11}^T(x_1,x_2,t) \;=\; \underbrace{\int_{-\infty}^{t} C(t-t')\,\frac{\partial}{\partial t'}\left\{\frac{P(t')}{A}\right\}dt'}_{\text{axial compressive strain } \epsilon_c} + \underbrace{\int_{-\infty}^{t} C(t-t')\,\frac{\partial}{\partial t'}\left\{\frac{P(t')\,w(x_1,t')\,x_2}{\rho^2 A}\right\}dt'}_{\text{bending strain } \epsilon_b} \tag{44}$$

where A is the cross sectional area and ρ the radius of gyration defined by $\rho^2 = I/A$. The creep compliance $C(t)$ it related to the relaxation modulus $E(t)$ through their LTs,

$$p\,\overline{C}(p) \;=\; \frac{1}{p\,\overline{E}(p)} \qquad \text{or} \qquad \int_0^t C(t-t')\,E(t')\,dt' \;=\; t \tag{45}$$

The region $t < t_1$ represents elastic conditions and and is the very early region of the relaxation modulus curve where $E(t) = E_0$ shown in Fig. 3. Creep buckling under whatever definition of critical times will occur at $t_{cr} > t_0$. At this point in time, the load has stabilized to a constant value P_0 since the loading has been completed at $t_1 < t_0$ in order to achieve initial elastic conditions. As time progresses the compressive strains and the bending strains both increase due to creep. The bending moment depends on the lateral deflection $w(x_1,t)$ and ϵ_b will increase in time at a greater rate than ϵ_c. Eventually, the tensile bending strain will exceed the axial compressive strain at one side of the column and e_{11}^T will begin to decrease (Fig. 23). Hence, one can define a critical time t_{cr}^{ϵ} as

$$\lim_{t\to t_{cr}^{\epsilon}}\left\{\frac{\partial \epsilon_{11}^T(x_1,x_2^{max},t)}{\partial t}\right\} \;=\; \frac{P_0}{A}\left[\lim_{t\to t_{cr}^{\epsilon}}\left\{\int_{-\infty}^{t}\frac{\partial C(t-t')}{\partial t}\,dt' \;+\; C(0)\right.\right.$$
$$\left.\left. -\int_{-\infty}^{t}\frac{\partial C(t-t')}{\partial t}\,\frac{w(x_1,t')\,x_2^{max}}{\rho^{*2}}\,dt' \;-\; C(0)\,w(x_1,t)\frac{x_2^{max}}{\rho^{*2}}\right\}\right] \;\to\; 0 \tag{46}$$

A similar approach has been used in [58] for establishing buckling stresses in elastic plates and in [7] for creep buckling of viscoelastic plates and can be applied to columns as well.

2.3.2 Creep buckling definition based on constant log deformation rates

An inspection of Figs. 24 and 25 show that after some time displacements, velocities and accelerations increase at constant rates on these semi-log plots. This condition occurs by virtue of Eq. (31) when the $r = 1$ term begins to be the dominant one for $\alpha_1 < 0$ and $\log[w(x_1, t)] \sim -\alpha_1 t$. The time at which the log of the deflections first acquires constant, i.e. time independent slopes is called here the pseudo creep buckling time t^*_{cr} and is defined as the first time when

$$\lim_{t \to t^*_{cr}} \left\{ \log \left[\frac{\partial w(x_1, t)}{\partial t} \right] \right\} \rightarrow \text{ constant} \tag{47}$$

Fig. 26 shows plots of t^*_{cr} for static and dynamic responses based on the two considered SLSs. Results will be discussed in detail in a subsequent section. In [58] a similar approach was used based on the intersection of the tangents of the straight portions of the strain vs. load plots for elastic plates, thus eliminating the curved parts of the curves. Neither approach is based on any rigorous theoretical considerations and must be viewed with caution.

2.3.3 Column survival definition based on material failure probability

Viscoelastic failure criteria, such as ultimate stresses, degrade in time independently of relaxation moduli and failures may occur before or after any creep buckling instabilities manifest themselves (Fig. 23). These are material failures which are independent of creep buckling and define the life time of the structure designated as t_{LF}. Consequently, t_{cr} may be greater, smaller or equal than t_{LF}. Indeed, in Refs. [29] [33] and [96] Shanley & Ryder's [91] interaction curve approach has been used to estimate failures under combined inelastic deterministic stresses.

Some failure mechanisms observed in composites are substantially different from those observed in metals [18], [32], [74], [84], [85], [105], as delamination is a phenomenon unique to composites (Fig. 28). From a design analysis point of view, one needs only to consider delamination onset because at that stage a flight structure has for all practical purposes failed, particularly if it is a light weight flight structure. In [18] an expression has been formulated for the temperature, moisture and time dependency of uniaxial composite failure stresses. An extensive review of available experimental composite failure data is presented in [42] where such data has been used to formulate deterministic and stochastic delamination failure analyses. Experimental results indicate that uniaxial deterministic delamination onset stresses in tension and shear obey laws of the type

$$\sigma^{\mathbf{F}}_{ij}(t) = \begin{cases} \sigma^{\mathbf{F}}_{ij0} & -\infty \le t \le t^{\mathbf{F}}_2 \\ \sigma^{\mathbf{F}}_{ij0} - D_{ij} \log\left(t/t^{\mathbf{F}}_4\right) & t^{\mathbf{F}}_2 \le t \le t^{\mathbf{F}}_3 \\ 0 & t \ge t^{\mathbf{F}}_3 \end{cases} \tag{48}$$

where all parameters are material, temperature, moisture and load (tension, shear, etc.) dependent.

In [43] deterministic and stochastic invariant combined load failure criteria have been developed in terms of two relations

$$\frac{1}{3} \sum_{i=1}^{q} \left[\frac{\widetilde{J}_i(x,t)}{\mathcal{J}_i(x,t)} \right]^{c_i} = \widetilde{V}(x,t) \tag{49}$$

$$\frac{1}{3} \sum_{i=1}^{q} \left[\frac{\widetilde{\mathcal{J}}_i(x,t)}{\mathcal{J}_i(x,t)} \right]^{c_i} = \widetilde{v}(x,t) \tag{50}$$

where J_i, $\mathcal{J}_i$ and c_i are mean values and random variables are indicated with a $\widetilde{\ }$. The upper summation limit q is the number uniaxial loads. Typical deterministic failure stress surfaces may be found in [43] and [46]. The applied and failure stress invariants are defined by

$$\widetilde{J}_1 = \widetilde{\sigma}_{ii} \qquad \widetilde{J}_2 = \widetilde{\sigma}_{ij}\,\widetilde{\sigma}_{ij} \qquad \widetilde{J}_3 = \widetilde{\sigma}_{ij}\,\widetilde{\sigma}_{ik}\,\widetilde{\sigma}_{kj} \tag{51}$$

$$\widetilde{\mathcal{J}}_1 = \widetilde{F}_{ii} \qquad \widetilde{\mathcal{J}}_2 = \widetilde{F}_{ij}\,\widetilde{F}_{ij} \qquad \widetilde{\mathcal{J}}_3 = \widetilde{F}_{ij}\,\widetilde{F}_{ik}\,\widetilde{F}_{kj} \tag{52}$$

where F_{ij} are uniaxial failure stresses.

Failure occurs whenever

$$\widetilde{U}(x,t) = \widetilde{V}(x,t) - \widetilde{v}(x,t) \leq 0 \tag{53}$$

For deterministic applied loads and random failure stresses, or vice versa, one needs only to apply one probability density function (PDF) to either Eq. (49) or (50). Ref. [32] presents an evaluation of experimental delamination data that can be represented by a Weibull type probability density function (PDF) [75], [76], [106]. Upon integrating this PDF, one obtains the failure probability $\widetilde{P}_F$ as

$$\widetilde{P}_F(x,t) = 1 - \exp\left\{-\left[\frac{\widetilde{U}(x,t)}{\kappa}\right]^{\gamma}\right\} \tag{54}$$

where the material property parameters γ and κ and their values were discussed in detail in [32] and [42]. Since for plate problems the stresses σ_b, σ_n and σ_s are functions of x and t, it follows that the failure probabilities $\widetilde{P}_F$ are also dependent on position within the plate and on time.

The time t_{LF} corresponding to the largest value of $\widetilde{P}$ at a point $x_i = c_i$ in a structure is the life time or survival time. It is defined by

$$\widetilde{P}(c, t_{LF}) = \max\left\{\widetilde{P}(x,t)\right\} \leq 1 \tag{55}$$

In stochastic probabilistic structural failure analysis, one seeks similar points or regions where $\widetilde{P}_F(x, t_{LF}) = 1$ or alternately the maximum probability value $\widetilde{P}_F(x, t_{LF}) < 1$ to indicate column survival probabilities under a prescribed load $P(t) < P_E$ and a given initial imperfection $w_o(x)$. A similar but distinct class of problems arises from the imposition of the specification of design survival times t_{LFD} each corresponding to a design failure probability $\widetilde{P}_{FD}(t_{LFD}) \leq 1$, or conversely the prescription of a t_{LFD} with an attendant $\widetilde{P}_{FD}(t_{LFD})$.

It must, of course, be remembered that the five decisive times listed in Table 5 (t_{cr}, t^{ϵ}_{cr}, t^{*}_{cr}, t_{LF}, t_{LFD}) are unrelated to each other and each represents a distinct definition of instability or failure conditions.

2.4 Computational protocols

Excellent comprehensive treatments of viscoelastic computational analyses and protocols maybe found in [77], [83], [94] and [97], to mention a only a few texts.

The present problem involves the solutions of the column and torsion real time governing differential-integral relations of Eq. (7). This can be accomplished in any one of the following ways:

1. In special cases (constant properties, loads, temperatures, etc.) Laplace or Fourier time transforms can be used [3], [4], [41].

2. In more complicated problems, a combination of spatial finite element and temporal finite difference or recurrence relation formulations is available [110], [111].

3. Galerkin's method [62] may be used to reduce the multidimensional spatially dependent PDE relations to temporal ODEs or integral-differential equations.

4. Alternately, the constitutive relations may be formulated in terms of differential operators as exemplified by the column governing relation (38). This system can be solved using a Runge-Kutta approach [68], [87] as seen from Eq. (66). The inherent difficulty with the differential constitutive relations is that characterization of real materials requires derivatives of orders between 20 and 30, the s values in in Eq. (35). The linear integral constitutive relations, on the other hand, have relaxation functions represented by Prony series [87], Eq. (6), where the character of the integral relations does not change as $N \sim s$ increases or decreases in value.

5. Integral ordinary differential equations may also be solved with a newly developed protocol [56] which serves to evaluate the constitutive relation integrals in Eq. (3) and (4). This removes the undesirable need to solve high order DEs stemming from the alternate DE constitutive relation forms. Additional and distinct numerical protocols may also be found in [98] and [113].

2.5 Illustrative examples for two specific viscoelastic materials

As a set of simple but meaningful examples consider the single Maxwell model (SMM) and the standard linear solid (SLS) [17], [38]. They represent the most primitive viscoelastic constitutive relations exhibiting Class I and II time behavior of Table 3. Their 1–D constitutive relations are defined by their relaxation moduli $E(t)$

$$\text{SMM} \Longrightarrow \; E(t) \;=\; \exp\left(-\frac{t}{\tau}\right) \tag{56}$$

$$\text{SLS} \Longrightarrow \; E(t) \;=\; \left[1 \,-\, \frac{\tau_2}{\tau_1}\right] \exp\left(-\frac{t}{\tau_1}\right) \;+\; \frac{\tau_2}{\tau_1} \tag{57}$$

The differential operators of the constitutive relations (35) for the SMM reduce to

$$\text{SMM} \Longrightarrow \; \mathcal{P} \;=\; \frac{\partial}{\partial t} \,+\, \frac{1}{\tau} \qquad \text{and} \qquad \mathcal{Q} \;=\; \frac{\partial}{\partial t} \qquad \text{with} \qquad \tau > 0 \tag{58}$$

while for the SLS they become

$$\text{SLS} \Longrightarrow \; \mathcal{P} \;=\; \frac{\partial}{\partial t} + \frac{1}{\tau_2} \qquad \text{and} \qquad \mathcal{Q} \;=\; \frac{\partial}{\partial t} + \frac{1}{\tau_1} \qquad \text{with} \quad \tau_1 > \tau_2 > 0 \tag{59}$$

resulting in the governing DEs

$$\left\{ \begin{array}{c} \text{SMM} \Longrightarrow \\ \\ \text{SLS} \Longrightarrow \end{array} \right\} \overbrace{\frac{d^3 W_r}{dt^3} \,+\, \underbrace{\frac{1}{\tau_2}}_{=\, A_{2r}} \frac{d^2 W_r}{dt^2}}^{\text{inertia terms}} \,+\, \underbrace{\left[\lambda_r^4 \,-\, D_r^{lf}(t)\right]}_{=\, A_{1r}(t)} \frac{dW_r}{dt}$$

$$+ \underbrace{\left\{ \begin{array}{c} -\,D_r^{lf}(t) \\ \hline \tau \\ \\ \dfrac{\lambda_r^4}{\tau_1} \,-\, \dfrac{D_r^{lf}(t)}{\tau_2} \end{array} \right\}}_{=\, A_{0r}(t)} W_r \;=\; \underbrace{\left\{ \begin{array}{c} 0 \\ \\ \dfrac{\lambda_r^4\, w_r^o}{\tau_1} \end{array} \right\}}_{=\, B_{0r}(t)} \qquad r = 1, 2, \cdots, R \quad \text{and} \quad t \geq 0 \tag{60}$$

Note that the governing DEs for these two distinct materials are similar except for the values of A_{0r} and B_{0r}. In the absence of inertia terms, both DEs have

solutions of the type

$$W_r(t) \;\sim\; \exp\left[\underbrace{-\int_{-\infty}^{t_1} \frac{A_{0r}(t')}{A_{1r}(t')}\,dt' - \frac{A_{0r}}{A_{1r}}(t-t_1)}_{=\,F_{Lr}(t,t_1)}\right] \tag{61}$$

For the SLS the argument of each exponential function becomes

$$\text{SLS} \Longrightarrow$$

$$F_{Lr}(t,t_1) \;=\; \underbrace{-\int_{-\infty}^{t_1} \left(\frac{r^2}{\tau_1} - \frac{e\,F_P(t')}{\tau_2}\right) \frac{dt'}{r^2 - e\,F_P(t')}}_{\text{transient loading}=F_{Tr}(t_1)} \underbrace{- \left(\frac{r^2}{\tau_1} - \frac{e}{\tau_2}\right) \frac{t-t_1}{r^2-e}}_{\substack{\text{steady state loading} \\ =\,F_{STr}(t,t_1)}}$$

$$r = 1, 2, \cdots, R \qquad \text{and} \qquad t > t_1 \tag{62}$$

The corresponding SMM F_{Lr} function can be obtained by setting $\tau = \tau_2$ and $\tau_1 = \infty$ in Eqs. (57) and (62).

For the deflection to increase with time, the function $F_{ST1}(t,t_1) > 0$. The smallest constraint is placed on the value of e when $r = 1$ and the following conditions must be satisfied

$$\left.\begin{array}{lllll} \text{if} & F_{T1} < 0 & \text{then} & F_{ST1} > |F_{T1}| > 0 \\ \text{if} & F_{T1} > 0 & \text{then} & F_{ST1} > 0 \end{array}\right\} \qquad t > t_1 \tag{63}$$

Therefore, in order for the deflection to increase with time one of the terms of the ratios A_{01}/A_{11} must be negative. For the SMM this does not present a problem since $-A_{01} < 0$ and $A_{11} > 0$. However, for the SLS, while the denominator is always positive, the numerator for $r = 1$ can be negative if and only if

$$\text{SLS} \Longrightarrow \quad 0 < \frac{\tau_2}{\tau_1} < e < 1 \qquad \text{with} \qquad \tau_1 > \tau_2 \quad \text{and} \quad r = 1 \tag{64}$$

Consequently for the SLS where the long time strains are bounded, only loads in the range $P < \tau_2 P_E/\tau_1 < P_E$, stemming from $r = 1$, will lead to creep buckling as defined by Eq. (1). Subsequent $W_r(t)$ terms of Eq. (15) where $r > 1$, will always mandate e values with larger lower bounds necessary to achieve creep buckling. These larger e values even if below unity are irrelevant, since the divergence of $w(x,t)$ with time will occur at any of the permissible e values for $r = 1$. For the Class I viscoelastic materials exhibiting unbounded long time strains, any load $P < P_E$ will lead to creep buckling with $w(t_{cr}) \to \infty$.

When inertia terms are included then the solution of Eqs. (60) becomes

$$W_r(t) \;=\; \sum_{q=1}^{3} B_{qr}\, e^{\alpha_{qr}\, t} \;+\; \frac{B_{0r}}{A_{0r}} \qquad r = 1, 2, \cdots, R \quad \text{and} \quad t > 0 \tag{65}$$

with $\alpha_{qr}t$ related to $F_{Lr}(t,t_1)$ as defined in Eqs. (61) and (62). The α_{qr} are readily identified as the roots of a third order algebraic equation and are listed in standard algebra texts. From a creep buckling point of view only those roots where $\Re\{\alpha_{qr}\} > 0$ are of interest, since the $\Re\{\alpha_{qr}\} < 0$ and the $\Im\{\alpha_{qr}\}$ parts each lead to stable finite displacements in time for $P < P_E$, such that $\lim_{t\to\infty} w(x,t) < \infty$.

Table 6: Parametric values for illustrative examples

Material	τ_1	τ_2	E_∞	ζ_{TH}	e	Fig. No.
SLS	.5	.25	.5	.5	.3, .6	4 – 13
SLS	.5	.05	.1	.1	.06, .12	14 – 17
SMM	∞	20	0	0	.3, .9	19 – 22

3. Discussion of results

Numerical solutions of Eq. (38) were obtained by employing a fourth order Runge-Kutta method, yielding $s+3$ coupled simultaneous ODEs of the form

$$\left.\begin{aligned} y_{1r}(t) &= W_r(t) \\ y_{2r}(t) &= \dot{y}_{1r}(t) \\ y_{3r}(t) &= \dot{y}_{2r}(t) \\ \vdots &= \vdots \\ y_{(s+2)r}(t) &= \dot{y}_{(s+1)r}(t) \\ y_{(s+3)r}(t) &= B_{0r} - a_{s-1}\, y_{(s+2)r}(t) - \sum_{n=0}^{s} A_{nr}(t)\, y_{(n+1)r}(t) \end{aligned}\right\} \tag{66}$$

The computations were carried out using MATLAB© on a MacBook Pro™.

Several illustrative solutions for simple SLS (Figs. 4 to 17) and SMM (Figs. 19 to 22) materials of Eqs. (60) have been carried out with load patterns described by Eqs. (1) and displayed in Fig. 1 . The loading interval $0 \le t \le t_1$ can, of course, be lengthened or shortened for increased or decreased relaxation times, provided the constraint $t_1 \le t_0$ is enforced. The four typically representative loads show significant differences between each other both in values as well as in shape. The relaxation moduli for the illustrative examples are shown in Fig. 3 and exhibit variations in τ and E_∞ values. Quasi-static and dynamic solutions for various values of the pertinent parameters as listed in Table 6 are displayed in these figures. For comparison purposes, all curves are normalized w.r.t. their individual maximum values.

Figs. 4 and 5 show SLS deflection results for Load B under quasi-static and dynamic conditions. The value of the threshold ζ and fully relaxed modulus E_∞ is .5, since both quantities are equal to τ_2/τ_1 for the present. Note the striking differences in responses for the quasi-static and dynamic cases. In both examples, the results clearly indicate, as predicted by the foregoing analysis, that the SLS column is stable for loads below the threshold ζ_{TH} values while exhibiting creep buckling as defined by Eqs. (1) for $e \ge \zeta_{TH}$.

Figs. 6 through 9 are composite plots for the SLS incorporating quasi-static and dynamic results of the two previous figures and showing their relation to the loading and moduli histories. The loadings are those of Loads A – D described in Eqs. (14) and they reach their maximum values at $t_1 < t_0$ when relaxation is initiated. For both sets of chosen τs in these illustrative examples, the dynamic motion decays and creep buckling occurs after the relaxation moduli have decreased to their respective long time fully relaxed values of E_∞. Value changes

in the various parameters of Eq. (7) will shift the deformation curves to the left or right (forward or backward in time) relative to the modulus curves. Detailed responses for each load, as well as the relaxation moduli, are depicted in Figs. 10 to 17.

The loading rise time t_1 is relatively short, since it must be less than the time t_0 when relaxation begins in order to achieve comparable elastic initial conditions. In the examples treated here it is four orders of magnitudes smaller than than t_R, the time when full relaxation of the modulus (E_∞) is realized. The influence of the various loads A – D over then entire relaxation is minimal, since the initial transients die out relatively quickly. However, the distinction in quasi-static and dynamic responses is readily visible from Figs. 6 and 17. In the loading range $e < \zeta_{TH}$ in particular, the quasi-static deflections rise to a steady state finite value, while the corresponding dynamic ones oscillate and damp out to zero. The foregoing represent typical Class II material column behavior.

Composite plots for the SMM under Loads A – D are shown in Fig. 18 and are derived from the detailed graphs of Figs. 19 to 22. For this Class I material the threshold $\zeta_{TH} = 0$ and creep buckling proceed under any load $0 < P < P_E$. Again it is seen that for the same reasons as stated above, the influence of the various Load shapes A – D is not discernible. This is equally true for longer loading periods, $t_1 = .001$ and .01 for the SLS and SMM respectively with relaxation times of .5 and 20.

The next series of figures (23 to 27) speak to the various protocols for creep buckling estimations. Fig. 23 is a typical set of curves showing bending and compressive strains in relation to the maximum lateral deflection. The strain reversal is unambiguously visible at $t^{\epsilon}_{cr} = .645$. The pseudo critical times t^{*}_{cr} are shown in Fig. 26 and are derived from plots of the type displayed in Figs. 24 and 25 and are subject to less precise visual inspection of departures from constant slopes. Note also that these changes in slopes occur at different times for deflections, velocities and accelerations (Fig. 24).

Fig. 27 represents critical times at various operating temperatures as a function load ratios e. These curves are being intersected by failure condition envelopes at the same temperatures. These crossing determine the lifetime or survival column times t_{LF} described previously and the failure condition determinations are outlined next.

The invariants of Eqs. (51) and (52) are based on the three distinct stresses present in viscoelastic columns, namely

$$\left.\begin{aligned} \text{compression:} \quad \sigma_c &= \frac{P(t)}{A} \\ \text{bending:} \quad \sigma_b &= \frac{P(t)\, w(x_1,t)\, x_2}{I} \\ \text{shear:} \quad \sigma_s &= \frac{1}{h}\int_{x_2}^{c} \frac{\partial \sigma_b(x_1, x_2^{'}, t)}{\partial x_2^{'}}\, h\, dx_2' \end{aligned}\right\} \tag{67}$$

and are

$$\widetilde{\mathcal{J}}_1 = |\sigma_c| + |\sigma_b| \qquad \widetilde{\mathcal{J}}_2 = (|\sigma_c| + |\sigma_b|)^2 + 2\,\sigma_s^2$$

$$\widetilde{\mathcal{J}}_3 = (|\sigma_c| + |\sigma_b|)^3 + |\sigma_s^3| + 3\,(|\sigma_c| + |\sigma_b|)^2\,|\sigma_s| + 3\,(|\sigma_c| + |\sigma_b|)\,\sigma_s^2 \tag{68}$$

with h and A respectively the column width and area.

Fig. 28 depicts experimental results for viscoelastic composites uniaxial tension and shear delamination onset stresses as reported by Dillard & Brinson 1983. These values and the Weibull failure distributions observed in the experiments reported in [32] together with the analytically derived applied stresses

are introduced into Eqs. (49) to (54), (67) and (68) to produce Figs. 27 to 30. The solutions displayed in Fig. 29 indicate the influence of higher temperatures, which serve to increase failure probabilities while decreasing survival times. From Fig. 30 it is seen that inertia contributions serve to increase failure probabilities and to decrease survival times under static loads, when compared to static column solutions.

The latter plots represent the ultimate goals of the present analyses as they relate material failure (delamination) and column bending with failure probabilities and survival times. Separate probabilistic analyses can also be introduced for the determination of viscoelastic stresses, strains and column deflections if moduli are modeled in terms of actual random properties and the stochastic analytical formulations in [39] are carried out. Under such procedures one is then confronted with two separate pairs of failure probabilities and survival times, i.e., one for creep buckling and the other for delaminations. Depending on these combinations, the shortest survival time and the highest failure probability will govern column life time design and predictions. The appropriate failure mode (buckling vs. delamination) will emerge as a by-product of the more general stochastic analysis.

Selection and use of viscoelastic material properties can, of course, be optimized with prescribed constraints on deformation, lifetime, or probability of failure, etc., as shown in [5], [16] and [40]. No optimization attempts were made here as the primary intend is to study dynamic effects on creep buckling.

With the current pervasive use of high polymer fiber composites in primary load carrying aerospace[3] structures, the use of viscoelastic analyses rather than elastic ones becomes ever more mandatory. Typical examples are wings, horizontal and vertical tail surfaces, fuselages, helicopter blades, high temperature metal turbine blades, wind turbine blades, etc.

4. Conclusions

Analytical formulations for and computational simulations of linear viscoelastic columns indicate that the inclusion of dynamic phenomena, which are predominantly caused by viscoelastic material properties rather than transient loading patterns, greatly alters resulting deformation patterns and stability results. However, very short time individual loading patterns do not affect deformations and creep buckling times. Furthermore, it is shown that columns and wings made of viscoelastic materials with finite long time strains do not creep buckle under either quasi-static or dynamic conditions unless axial loads/aerodynamic torques exceed a lower bound which depends solely on viscoelastic material parameters and is unaffected by loading paths and column dimensions.

Since neither quasi-static nor dynamic linear viscoelasticity lead to formal analytic creep buckling/divergence times, alternate definitions were explored. Unfortunately, these procedures do not yield equal critical time results. However, the strain reversal method is the most realistic and physically defensible one for columns. Similarly, approaches imposing finite limits on angles of twist are best suited for viscoelastic torsional divergence definitions.

Acknowledgement

Support by grants from the Private Sector Program (PSP) Division of the National Center for Supercomputing Applications (NCSA) at the University of Illinois at Urbana-Champaign (UIUC) is gratefully acknowledged.

[3] airplanes, UAVs, MAVs, missiles, space vehicles, jet engine blades, etc.

Dedication

This paper is dedicated with much love to my dear wife Lois Grimason-Hilton who steadfastly and patiently supports my continuing professional endeavors after retirement.

References

[1] Atanackovic, Teodor M. (1997) *Stability Theory of Elastic Rods.* World Scientific, Singapore.

[2] Bažant, Zdeněk P. and Luigi Cedolin (1991) *Stability of Structures - Elastic, Inelastic, Fracture and Damage Theories.* Oxford University Press, New York.

[3] Beldica, Cristina E., Harry H. Hilton and Sung Yi (1998a) "A sensitivity study of viscoelastic, structural and piezoelectric damping for flutter control," *Proceedings 39th AIAA/ASME/ASCE/AHS/ASC Structures, Structural Dynamics and Materials Conference, AIAA Paper 98-1848.* **2**:1304–1314.

[4] Beldica, Cristina E., Harry H. Hilton and Sung Yi (1998b) "Viscoelastic damping and piezo-electric control of structures subjected to aerodynamic noise," *Proceedings of the 4th AIAA/ CEAS Aeroacoustics Conference, AIAA Paper 98-2343.* **2**:805–815.

[5] Beldica, Cristina E. and Harry H. Hilton (1999a) "Piezoelectric control of linear viscoelastic columns - creep buckling and delaminations," *Proceedings of the 26th American Society of Composites Conference* (J. M. Whitney, ed.) 571–586.

[6] Beldica, Cristina E. and Harry H. Hilton (1999b) "Analytical simulations of optimum anisotropic linear viscoelastic damping properties," *Journal of Reinforced Plastics and Composites* **18**:1658 –1676.

[7] Beldica, Cristina E. and Harry H. Hilton (2000) "Delay of creep buckling and of probabilistic failures of linear viscoelastic plates," *Proceedings of the AIAA Structures, Structural Dynamics and Materials Conference, AIAA Paper 2000-1648* 129–138.

[8] Beldica, Cristina E. and Harry H. Hilton (2001) "Nonlinear viscoelastic beam bending with piezoelectric control - analytical and computational simulations," *Journal of Composite Structures* **51**:195–203.

[9] Bisplinghoff, Raymond L., Holt Ashley and Robert L. Halfman (1955) *Aeroelasticity.* Addison-Wesley Publishing Company, Cambridge, MA. (1980) Dover Publications, New York.

[10] Bleich, Friedrich (1952) *Buckling Strength of Metal Structures.* McGraw-Hill, New York.

[11] Bolotin, Vladimir V. (1964) *The Dynamic Stability of Elastic Systems.* Holden-Day, Inc., San Francisco.

[12] Bolotin, Vladimir V. (1995) "Dynamic stability of structures," *Nonlinear Stability of Structures: Theory and Computational Techniques.* (A. N. Kounadis & W. B. Krätzig, eds.) 1–72.

[13] Brinson, Hal F. and L. Catherine Brinson (2008) *Polymer Engineering Science and Viscoelasticity: An Introduction.* Springer, New York.

[14] Buckmaster, John D. (1973) "The buckling of thin viscous jets," *Journal of Fluid Mechanics* **61**:449–463.

[15] Buckmaster, Jodn D., Nachman, A. and L. Ting (1975) "The buckling and stretching of a viscida," *Journal of Fluid Mechanics* **69**:1–20.

[16] Cao, X. S. and Mlejnek, H.P. (1995) "Computational prediction and redesign for viscoelastically damped structures," *Computer Methods in Applied Mechanics and Engineering* **125**:1–16.

[17] Christensen, Richard M. (1982) *Theory of Viscoelasticity – An Introduction, 2nd Ed.* Academic Press, New York.

[18] Dillard, D. A. and Brinson, Hal F. (1983) "A numerical procedure for predicting and delayed failures in laminated composites," *Long Term Behavior of Composites*, (ed. T. K. O'Brien), *ASTM STP 813.* 23–37.

[19] Dillon, Jr., Oscar W. (1962) "Effect of variation of viscosity on creep deflections of columns," *Proceedings Fourth US National Congress on Applied Mechanics*, **2**:919–930, ASME, New York.

[20] Drozdov, Aleksey D. and Vladimir B. Kolmanovskii (1994) *Stability in Viscoelasticity.* Elsevier, Amsterdam.

[21] Dowell, Earl H. and Marat Ilganov (1988) *Studies in Nonlinear Aeroelasticity.* Springer, New York.

[22] Dowell, Earl H., Robert Clark, David Cox, Howard C. Curtis Jr., John W. Edwards, Kenneth C. Hall, David A. Peters, Robert H. Scanlan, Emil Simiu, Fernado Sisto and Thomas W. Starganac (2004) *A Modern Course in Aeroelasticity.* 4þ ed., Kluwer Academic Publishers, Boston.

[23] Elishakoff, Isaac, Yiwei Li and James H. Starnes, Jr. (2001) *Non-classical Problems in the Theory of Elastic Stability.* Cambridge University Press, Cambridge, UK.

[24] Engesser, Franz (1885) "Die Sicherung offener Brücken gegen Ausknicken," *Zentralblatt der Bauerverwaltung* **5**:71–72.

[25] Euler, Leonard (1744) "Additamentum I de curvis elasticis, methodus inveniendi lineas curvas maximi minimivi proprietate gaundentes," *Opera Omnia I* **24**:23–297.

[26] Freudenthal, Alfred M. (1950) *The Inelastic Behavior of Engineering Materials and Structures.* John Wiley & Sons, New York.

[27] Gerard, George (1952) "Note on creep buckling of columns," *Journal of the Aeronautical Sciences* **19**:714.

[28] Gerard, George (1956) "A creep buckling hypothesis," *Journal of the Aeronautical Sciences* **23**:879 –882, 887.

[29] Gerard, George (1962) *Introduction to Structural Stability Theory.* McGraw-Hill, New York.

[30] Gilat, Rivka and Jacob Aboudi (2002) "The Lyapunov exponents as a quantitative criterion for the dynamic buckling of composites plates," *International Journal of Solids and Structures* **39**:467–481.

[31] Heldenfels, Richard R. and Eldon E. Mathauser (1956) "A summary of NACA research on the strength and creep of aircraft structures at elevated temperatures," *NACA Research Memorandum L56D06.*

[32] Hiel, C. C., M. Sumich and D. P. Chappell (1991) "A curved beam test specimen for determining the interlaminar tensile strength of a laminated composite," *Journal of Composite Materials* **25**:854–868.

[33] Hilton, Harry H. (1952) "Creep collapse of viscoelastic columns with initial curvature," *Journal of the Aeronautical Sciences* **19**:844–846.

[34] Hilton, Harry H. (1957) "Pitching instability of rigid lifting surfaces on viscoelastic supports in subsonic or supersonic potential flow," *Advances in Solid Mechanics* 1–19, Edward Bros., Ann Arbor.

[35] Hilton, Harry H. (1958) "On the reduction of maximum loads in nonlinear viscoelastic columns," *Journal of the Aeronautical Sciences* **25**:399–400.

[36] Hilton, Harry H. (1960) "The divergence of supersonic, linear viscoelastic lifting surfaces, including chordwise bending," *Journal of the Aero/Space Sciences* **27**:926–934.

[37] Hilton, Harry H. (1961) "On the nonexistence of finite critical times for generalized linear viscoelastic columns with arbitrary initial curvatures," *Journal of the Aero/Space Sciences* **28**:655 –656.

[38] Hilton, Harry H. (1964) "An introduction to viscoelastic analysis," *Engineering Design for Plastics* (E. Baer, ed.) 199–276. Reinhold Publishing Corp., New York.

[39] Hilton, Harry H., John Hsu and John S. Kirby (1991) "Linear viscoelastic analysis with random material properties," *Journal of Probabilistic Engineering Mechanics* **6**:57–69.

[40] Hilton, Harry H. and Sung Yi (1992a) "Analytical formulation of optimum material properties for viscoelastic damping," *Journal of Smart Materials and Structures* **1:**113–122.

[41] Hilton, Harry H. and Sung Yi (1992b) "Anisotropic viscoelastic finite element analysis of mechanically and hygrothermally loaded composites," *International Journal of Composites Engineering* **3**:123–135.

[42] Hilton, Harry H. and Sung Yi (1993) "Stochastic viscoelastic delamination onset failure analysis of composites," *Journal of Composite Materials* **27**:1097–1113.

[43] Hilton, Harry H. and S. T. Ariaratnam (1994) "Invariant anisotropic large deformation deterministic and stochastic combined load failure criteria," *International Journal of Solids and Structures* **31**:3285–3293.

[44] Hilton, Harry H., Sung Yi and Michael J. Danyluk (1995) "Stochastic delamination buckling of composite viscoelastic columns," *Proceedings Second International Computational Stochastic Mechanics Conference*, (P. D. Spanos, Ed.) A. A. Balkema, Rotterdam, 687–696.

[45] Hilton, Harry H. and Sung Yi (1996) "Stochastic delamination onset of large deformation elastic and viscoelastic columns with follower loads," *Proceedings Seventh International Conference on Applications of Statistics and Probability* (M. Lemaire, J-L. Favre and A. Mébarki, eds.) **3**:1491–1495, A. A. Balkema, Rotterdam.

[46] Hilton, Harry H., Sung Yi and Michael J. Danyluk (1997a) "Probabilistic analysis of delamination onset in linear anisotropic elastic and viscoelastic composite columns," *International Journal of Reliability Engineering & System Safety* **56**:237–248.

[47] Hilton, Harry H., Jack R. Vinson and Sung Yi (1997b) "Anisotropic piezo-electro-thermo-viscoelastic theory with applications to composites," *Proceedings of the 11th International Conference on Composite Materials* **VI**:4881–4890, Gold Coast, Australia.

[48] Hilton, Harry H., Sung Yi, Jack R. Vinson and Chong Hin Koh (1998) "Probabilistic structural integrity of piezoelectric viscoelastic composite structures," *Proceedings of the ONR US - Pacific Rim Workshop on Composite Materials for Ship and Offshore Structures*, Honolulu.

[49] Hilton, Harry H. and Sung Yi (1999) "Creep divergence of nonlinear viscoelastic lifting surfaces with piezoelectric control," *Proceedings of the Second International Conference on Nonlinear Problems in Aviation and Aerospace* (S. Sivasundaram, ed.) **1**:271–280, European Conference Publications, Cambridge, UK.

[50] Hilton, Harry H. (2002) "Probabilistic delamination onset analysis of nonlinear anisotropic elastic and viscoelastic composite columns with large deformations," *Proceedings 43rd AIAA/ASME/ASCE/AHS Structures, Structural Dynamics and Materials Conference, AIAA Paper 2002-1713,* **5**:3423–3433.

[51] Hilton, Harry H. and Mohamed Achour (2003) "Probabilistic failure and survival time analysis of dynamic creep buckling of viscoelastic columns with large deformations and follower loads," *Proceedings 44th AIAA/ASME/ASCE/AHS Structures, Structural Dynamics and Materials Conference, AIAA Paper 2003-1915*, 3427–3437.

[52] Hilton, Harry H. (2006) "Dynamic thermal stress creep buckling, probabilistic failures and survival times of viscoelastic columns with follower loads," *Collected Papers in Structural Mechanics Honoring Dr. James H. Starnes, Jr., Special NASA/TM 2006-214276*, (N. F. Knight, N. P. Nemeth and J. B. Malone, eds.) 469–487, NASA Langley Research Center, VA.

[53] Hilton, Harry H. (2006) "Designer linear viscoelastic material properties tailored to minimize probabilistic failures or thermal stress induced dynamic column creep buckling," *Journal of Thermal Stresses* **29**:403–421.

[54] Hilton, Harry H. (2010) "Aeroelasticity and aero-viscoelasticity: a critical appreciation of similarities and differences," *Proceedings Fifty-first AIAA/ASME/ASCE/AHS/ASC Structures, Structural Dynamics and Materials (SDM) Conference, AIAA Paper 2010-2702*, Orlando.

[55] Hilton, Harry H. (2011) "Equivalences and contrasts between thermoelasticity and thermo-viscoelasticity: a comprehensive critique," *Journal of Thermal Stresses* **34**:488–535. DOI: 10.1080/01495739.2011.564010

[56] Hilton, Harry H. and Germain Sossou (2012) "Computational protocols for viscoelastic Prony series hereditary integrals and for variable coefficient integral-differential equations," *Submitted to Journal of Numerical Methods in Engineering.*

[57] Hodges, Dewey H. and G. Alvin Pierce (2002) *Introduction to Structural Dynamics and Aeroelasticity.* Cambridge University Press, New York.

[58] Hoff, Nicholas J., Bruno A. Boley and John A. Coan (1948) "The development of a technique for testing stiff panels in edgewise compression," *Proceedings of the Society for Experimental Stress Analysis* **5**(2):14–24.

[59] Hoff, Nicholas J. (1949) "Dynamic criteria of buckling," *Symposium on Engineering Structures,* A. G. Pugsley and D. R. Rexworthy, eds., 121–139, Butterworth, London.

[60] Hoff, Nicholas J. (1951) "The dynamics of the buckling of elastic columns," *ASME Journal of Applied Mechanics* **58**:3–52.

[61] Hoff, Nicholas J. (1954) "Buckling and stability," *Journal of the Royal Aeronautical Society* **18**:68–74.

[62] Hoff, Nicholas J. (1956) *The Analysis of Structures.* John Wiley & Sons, New York.

[63] Jahsman, W. E. and F. A. Field (1962) "Comparison of theoretical and experimental creep buckling times of initially straight, centrally loaded columns," *Journal of the Aerospace Science,* **29**:431–433,467.

[64] Jones, David I. G. (2001) *Handbook of Viscoelastic Vibration Damping.* John Wiley & Sons, New York.

[65] Jones, Robert M. (2006) *Buckling of Bars, Plates and Shells.* Bull Ridge Publishing, Blacksburg, VA.

[66] Kachanov, L. M. (1988) *Delamination Buckling of Composite Materials.* Kluwer Academic Publishers, Boston.

[67] Kempner, Joseph and Frederick V. Pohle (1953) "On the non-existence of a finite critical time for linear viscoelastic columns," *Journal of the Aeronautical Sciences* **20**:572–573.

[68] Kutta, Martin W. (1901) "Beitrag zur näherungsweisen Integration totaler Differentialgleichungen," *Zeitschrift der Mathematischen Physik* **46**:435–453.

[69] Lazan, Benjamin J. (1968) *Damping of Materials and Members in Structural Mechanics.* Pergamon Press, Oxford.

[70] Leipholz, Horst H. E. (Ed.) (1972) *Stability.* University of Waterloo Press, Waterloo, Ontario.

[71] Leipholz, Horst H. E. (1975) *Six Lectures on Stability of Elastic Systems.* University of Waterloo Press, Waterloo, Ontario.

[72] Leipholz, Horst H. E. (1980) *Stability of Elastic Systems.* Sijthoff & Noordhoff, Alphen aan den Rijn.

[73] Libove, Charles (1952) "Creep buckling of columns," *Journal of the Aeronautical Sciences* **19**:459–467.

[74] Lifshitz, J. M. and A. Rotem (1970) "Time-dependent longitudinal strength of unidirectional fibrous composites," *Fibre Science and Technology* **3**:1–20.

[75] Lin, Y. K. (1976) *Probabilistic Theory of Structural Dynamics.* Krieger Publishing Company, Huntington, NY.

[76] Lindquist, E. S. (1994) "Strength of materials and the Weibull distribution," *Journal of Probabilistic Engineering Mechanics* **9**:191–194.

[77] Marques, Severino P. C. and Guillermo J. Creus (2012) *Computational Viscoelasticity.* Springer, New York.

[78] Merrett, Craig G. and Harry H. Hilton (2011) "Flutter initiation under steady-state and accelerated free stream velocities," *SAE 2011 AeroTech Congress, SAE Paper 2011-01-2785*, Toulouse, France. DOI: 10.4271/2011-01-2785 *SAE International Journal of Aerospace* **4**:1449–1464.

[79] Merrett, Craig G. and Harry H. Hilton (2012) "The influence of unsymmetrical bending and torsion on elastic and viscoelastic wing flutter," *Proceedings Fifty-third AIAA/ ASME/ASCE/AHS/ASC Structures, Structural Dynamics and Materials (SDM) Conference, AIAA Paper ID 1212780*, Honolulu, HI, 2012.

[80] Merrett, Craig G. and Harry H. Hilton (2011) "Influences of starting transients, aerodynamic definitions and boundary conditions on elastic and viscoelastic wing and panel flutter," *Journal of Mathematics, Engineering, Science and Aerospace* **2**:121–144.

[81] Nashif, Ahid D., David I. G. Jones and John P. Henderson (1985) *Vibration Damping.* John Wiley & Sons, NY.

[82] Nguyen, Quoc Son (2000) *Stability and Nonlinear Solid Mechanics.* John Wiley & Sons, New York.

[83] Owens, R. G. and T. N. Phillips (2002) *Computational Rheology.* Imperial College Press London.

[84] Phoenix, S. L. (1979) "Statistical aspects of failure of fibrous materials," *Composite Materials: Testing and Design, ASTM STP 674*, (S. W. Tsai, Ed.), 455–483.

[85] Phoenix, S. L. and L-J. Tierney (1982) "A statistical model for the time dependent failure of unidirectional composite materials under local elastic load-sharing among fibers," *Engineering Fracture Mechanics* **18**:193–215.

[86] Post, Emil L. (1930) "Generalized differentiation," *Transactions American Mathematical Society* **32**:723–781.

[87] Prony, Gaspard C. F. R., Baron de (1795) "Essai experimental et analytique," *Journal de l'École Polytechnique de Paris* **1**:24–76.

item Runge, Carl (1895) "Über die numerische Auflösung von Differentialgleichungen," *Mathematische Analyse* **46**:167–178.

[88] Salençon, Jean (1988) *Méchanique des millieux continus.* Ellipses, Paris.

[89] Scanlan, Robert H. and Robert Rosenbaum (1951) *Introduction to the Theory of Aircraft Vibration and Flutter.* The Macmillan Co., New York.

[90] Schapery, Richard A. (1962) "Approximate methods of transform inversion for viscoelastic stress analysis," *Proceedings of the Fourth U. S. National Congress of Applied Mechanics* **2**:1075–1085.

[91] Shanley, Francis R. and Ryder, E. I. (1937) "Stress Ratios: The Answer to the Combined Loading Problem," *Aviation* **36**:28–29, 43, 66, 69–70.

[92] Shanley, Francis R. (1946) "Inelastic column buckling," *Journal of the Aeronautical Sciences* **14**:261–268.

[93] Shanley, Francis R. (1952) *Weight–Strength Analysis of Aircraft Structures.* McGraw-Hill, New York.

[94] Simo, Juan C. and Thomas J. R. Hughes (1998) *Computational Inelasticity.* Springer, New York.

[95] Singer, Josef, Johann Arbocz and Tanchum Weller (1998) *Buckling Experiments: Experimental Methods in Buckling of Thin-walled Structures.* Wiley, New York.

[96] Steinbacker, Franz R. and George Gerard (1952) *Aircraft Structural Mechanics.* Pitman Publishing Co., New York.

[97] Le Tallec, Patrick (1990) *Numerical Analysis of Viscoelastic Problems.* Springer-Verlag, Berlin.

[98] Taylor, Robert L., Karl L. Pister and G. L. Goudreau (1970) "Thermomechanical analysis of viscoelastic solids," *International Journal for Numerical Methods in Engineering* **2**:45–59.

[99] Torquato, Salvatore (2001) *Random Heterogeneous Materials: Microstructure and Macroscopic Properties.* Springer-Verlag, New York.

[100] Troger, Hans and Alois Steindl (1991) *Nonlinear Stability and Bifurcation Theory for Engineers and Applied Scientists.* Springer-Verlag, New York.

[101] Van Loan, Charles F. (1992) *Computational Frameworks for the Fast Fourier Transform.* SIAM, Philadelphia.

[102] Vinogradov, Aleksandra M. (1985) "Nonlinear effects in creep buckling analysis of columns," *Journal of Engineering Mechanics, ASCE* **111**:757–767.

[103] Vinogradov, Aleksandra M. (1987) "Buckling of viscoelastic beam columns," *AIAA Journal* **25**: 479–483.

[104] von Kármán, Theodore (1908) "Die Knickfestigkeit gerader Stäbe," *Physikalische Zeitschrift* **9**:136 –140.

[105] Watson, A. S. and R. L. Smith (1985) "An examination of statistical theories for fibrous materials in the light of experimental data," *Journal of Materials Science* **20**:3260–3270.

[106] Weibull, Waloddi (1951) "A statistical distribution function of wide applicability," *ASME Journal of Applied Mechanics* **18**:293–297.

[107] Wilson, Dale W. and Jack R. Vinson (1984) "Viscoelastic analysis of laminated plate buckling," *AIAA Journal* **22**:982–988.

[108] Wilson, Dale W. and Jack R. Vinson (1985) "Viscoelastic buckling analysis of laminated composite columns," *Recent Advances in Composites in the United States and Japan, ASTM STP 864* (J. R. Vinson and M. Taya, eds.), 368–383. ASTM, Philadelphia.

[109] Wright, Jan R. and Jonathan E. Cooper (2007) *Introduction to Aircraft Aeroelasticity and Loads.* John Wiley, Hoboken, NJ.

[110] Yi, Sung and Harry H. Hilton (1994) "Dynamic finite element analysis of viscoelastic composite plates in the time domain," *International Journal for Numerical Methods in Engineering* **37**:4081–4096.

[111] Yi, Sung, S. F. Ling, M. Ying, Harry H. Hilton and Jack R. Vinson (1999) "Finite element formulation for anisotropic coupled piezo-hygro-thermo-viscoelastic dynamic problems," *International Journal of Numerical Methods in Engineering* **45**:1531–1546.

[112] Yi, Sung, Kerm Sin Chan and Harry H. Hilton (2002) "Nonlinear viscoelastic finite element analyses of thermosetting polymetric composites during cool-down after curing," *Journal of Composite Materials* **6**:3–17.

[113] Zak, Adam R. (1968) "Structural analysis of realistic solid propellant materials," *Journal of Spacecraft* **5**:270–275.

Appendix A – Evaluation of lts of the $C_r(t)$ functions

Consider the LT of the loading function $F_P(t)$, which in turn defines the $C_r(t)$ function of Eqs. (17)

$$\frac{\overline{C}_r(p)}{e\,P_r^*} = \int_0^{t_1} F_P(t)\,e^{-pt}\,dt + \frac{e^{-p\,t_1}}{p} = \overline{F}_P(p,t_1) + \frac{e^{-p\,t_1}}{p} \qquad (0 \le p \le \infty) \quad (69)$$

where $\overline{F}_P(p,t_1)$ depends on the definition of the applied loads as prescribed by Eq. (14) their LTs become

$$\frac{\overline{C}_r(p)}{e\,P_r^*} = \left\{ \begin{array}{ll} \overline{F}_A(p,t_1) & \text{Load A} \\ \overline{F}_B(p,t_1) = \dfrac{1}{2\,p}\left[e^{-p\,t_1} + \dfrac{\pi^2 - 2\,\pi\,t_1\,p}{4\,p^2\,t_1 + \pi^2}\right] & \text{Load B} \\ \overline{F}_C(p,t_1) = \dfrac{1}{p} & \text{Load C} \\ \overline{F}_D(p,t_1) = \dfrac{e^{-p\,t_1}}{p^2} & \text{Load D} \end{array} \right\} \qquad (70)$$

with $C_{r\infty}/eP_r^* = 1$ for Loads A through D and where

$$\overline{F}_A\,(p,t_1) = \frac{-4\,t_1\,e^{-p\,t_1}}{\left[4\,p^2\,t_1^2 + \pi^2\right]^3}\left[-2\pi^4 + 32\,p^3\,t_1^3 + 8\,t_1^3\,p^3\,\pi^2 + 32\,p^4\,t_1^4 + t_1\,p\,\pi^4\right.$$

$$\left. +16\,t_1^5\,p^5 - 24\,p\,t_1\,\pi^2\right] + \frac{16\,\pi\,t_1\left(12\,p^2\,t_1^2 - \pi^2\right)}{\left[4\,p^2\,t_1^2 + \pi^2\right]^3} + \frac{e^{-p\,t_1}}{p} \qquad (71)$$

It is to be noted that the term $C_r(t)$ primarily depends on the load function $P(t)$ of Eq. (17) and that its long term behavior is insensitive to the relatively very short time initial ramp loading functions of Eqs. (14).

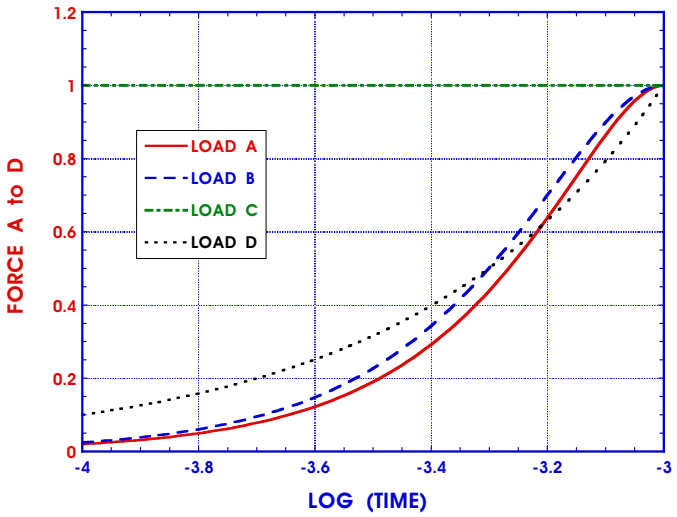

Figure 1: Transient and steady-state loading functions

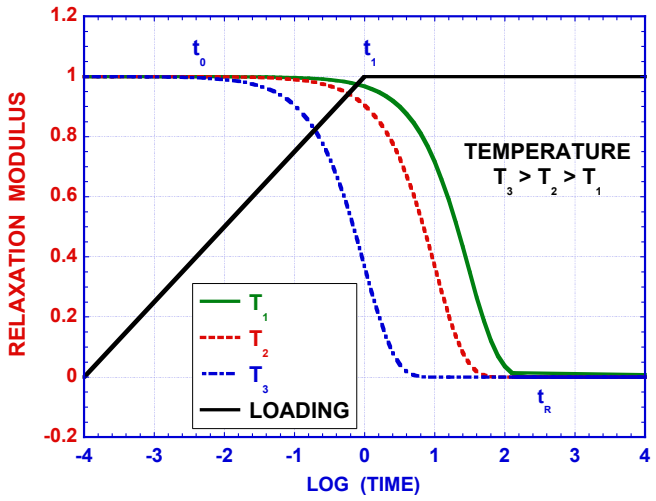

Figure 2: Loading and relaxation functions

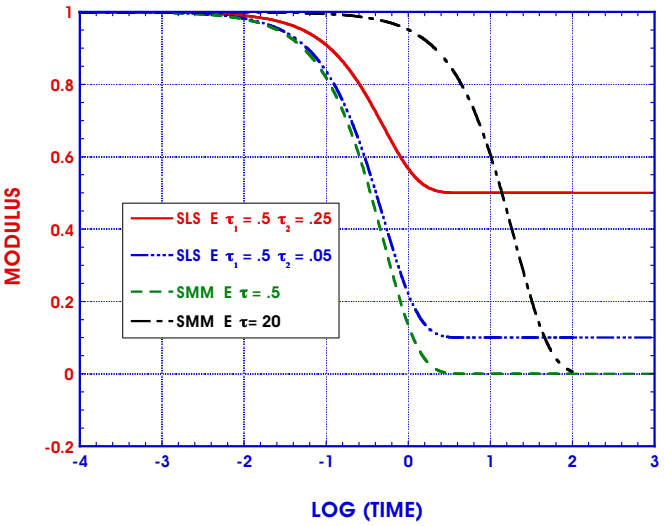

Figure 3: SLS and SMM relaxation moduli

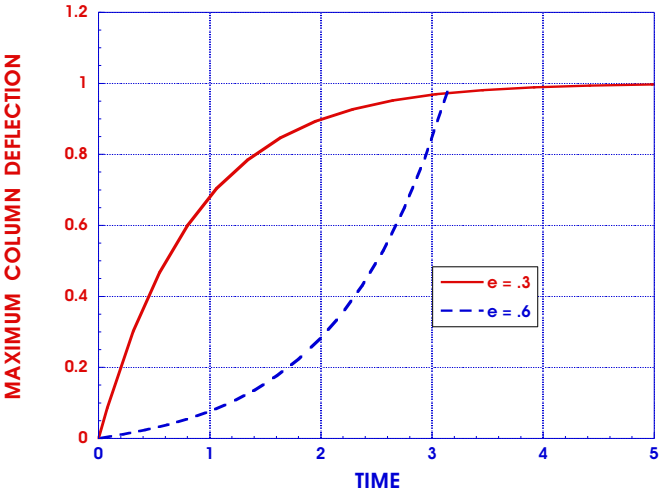

Figure 4: Quasi-static deflections for $\tau = .5$ & .25, e = .3 & .6

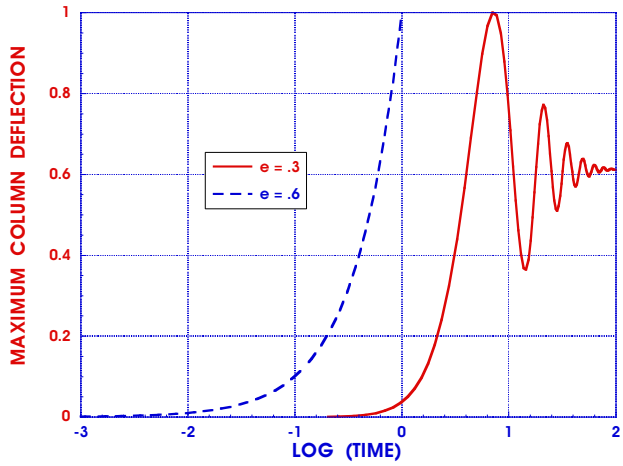

Figure 5: Dynamic response for $\tau = .5$ & $.25$, e = .3 & .6

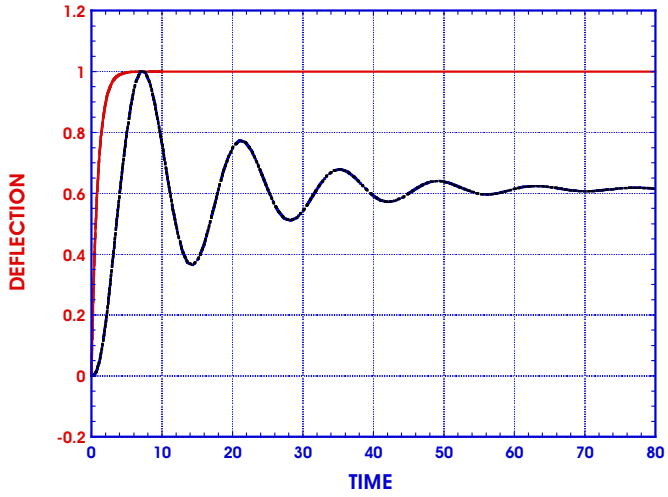

Figure 6: Quasi-static and dynamic deflections for for $e = .3, \tau_1 = .5, \tau_2 = .25$, loads A – D

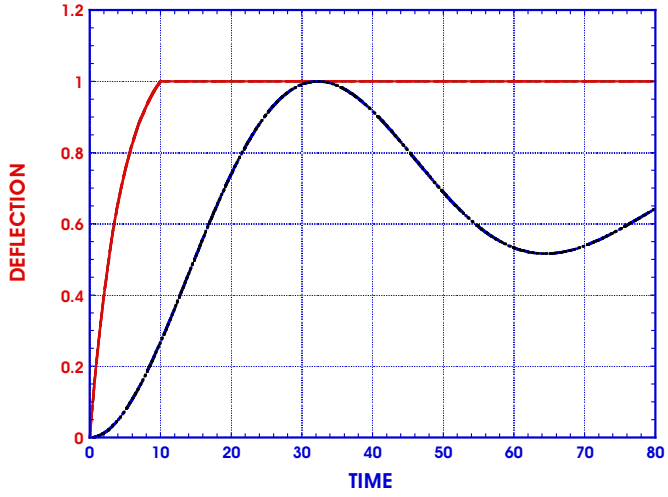

Figure 7: Quasi-static and dynamic deflections for $e = .09, \tau_1 = .5, \tau_2 = .05$, loads A – D

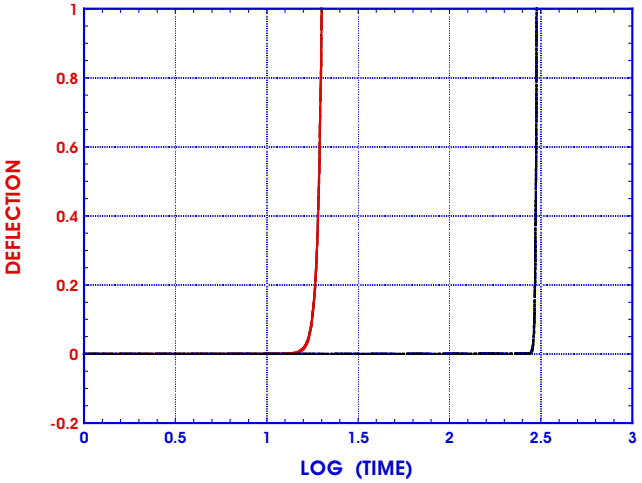

Figure 8: Quasi-static and dynamic unstable deflections for $e = .6, \tau_1 = .5, \tau_2 = .25$, loads A - D

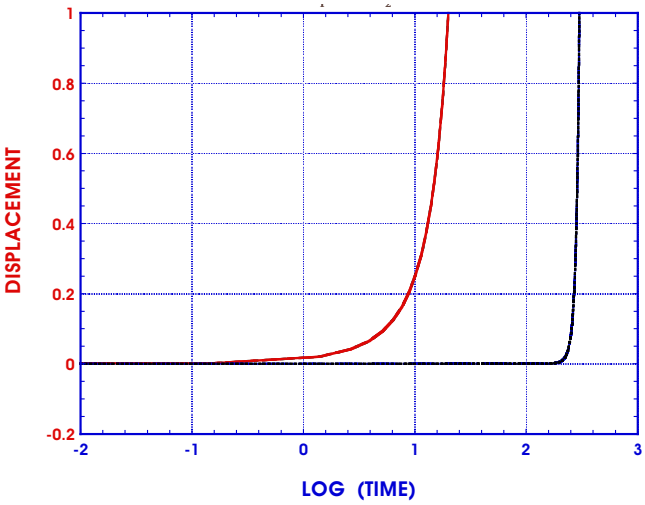

Figure 9: Composite static/dynamic for $e = .105, \tau_1 = .5, \tau_2 = .05$, loads A - D

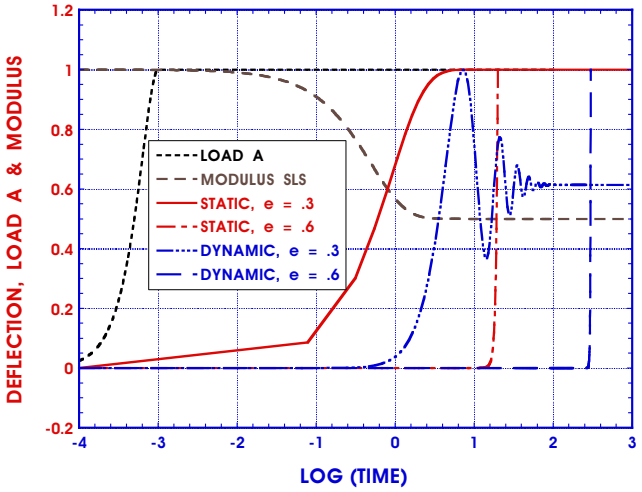

Figure 10: Quasi-static and dynamic deflections for $\tau_1 = .5, \tau_2 = .25$, load A

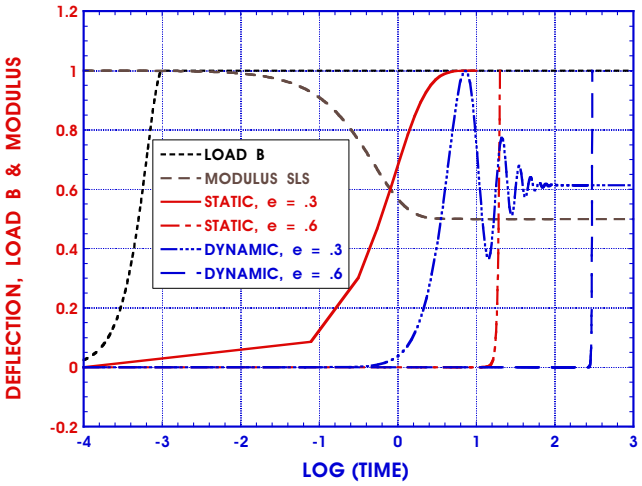

Figure 11: Quasi-static and dynamic deflections for $e = .3$ and 6, load B

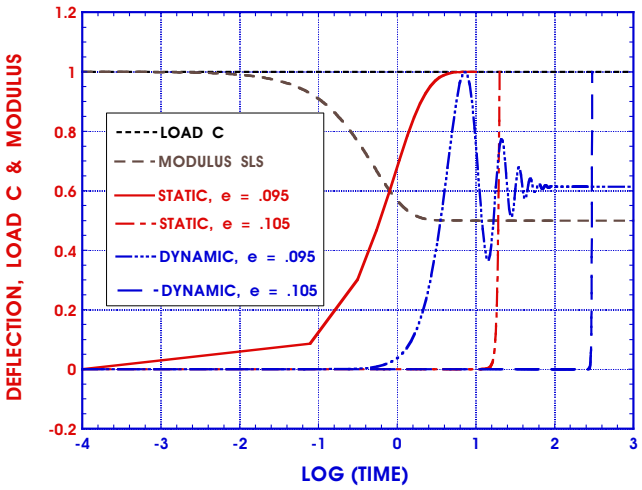

Figure 12: Quasi-static and dynamic deformations for $e = .095$ and .105, load C

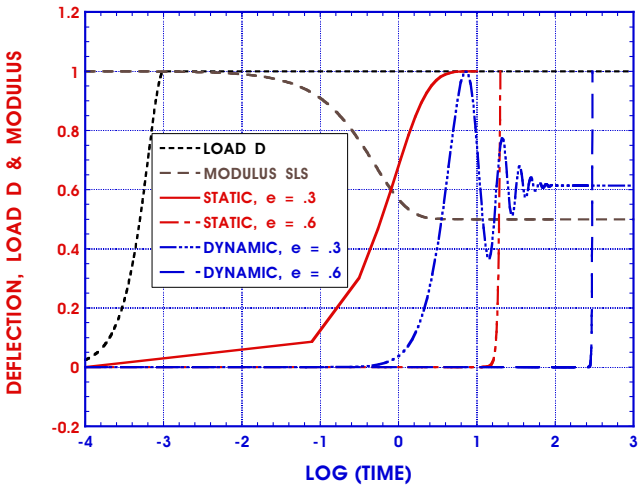

Figure 13: Quasi-static and dynamic deformations for $e = .3$ and .6, $\tau_1 = .5$, $\tau_2 = .05$, load D

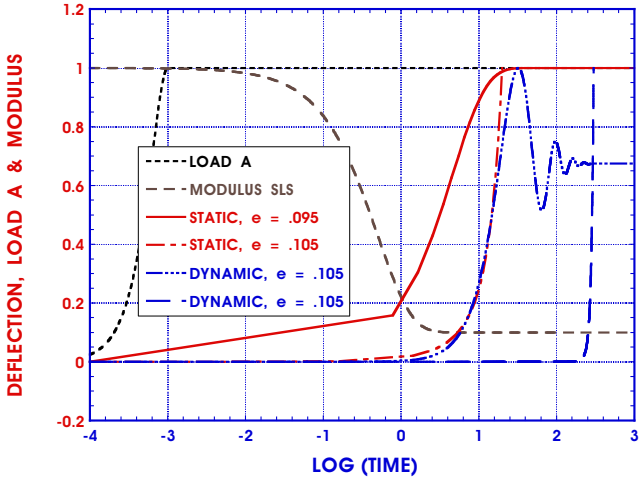

Figure 14: Quasi-static and dynamic deformations for $e = .095$ and .105, $\tau = .5$ and .05, load A

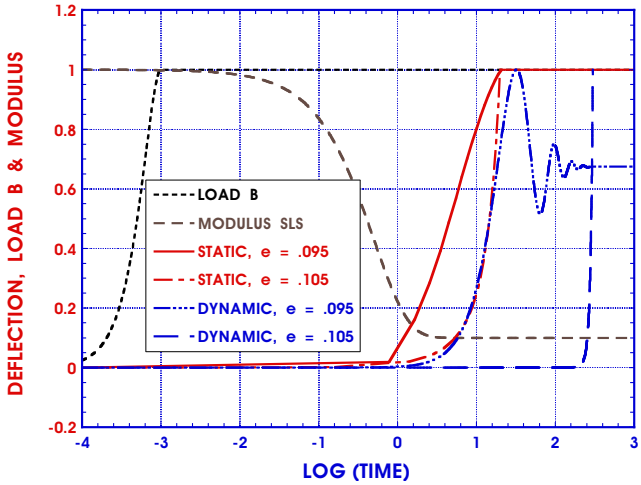

Figure 15: Quasi-static and dynamic deformations for $e = .095$ and .105, $\tau_1 = .5, \tau_2 = .05$, load B

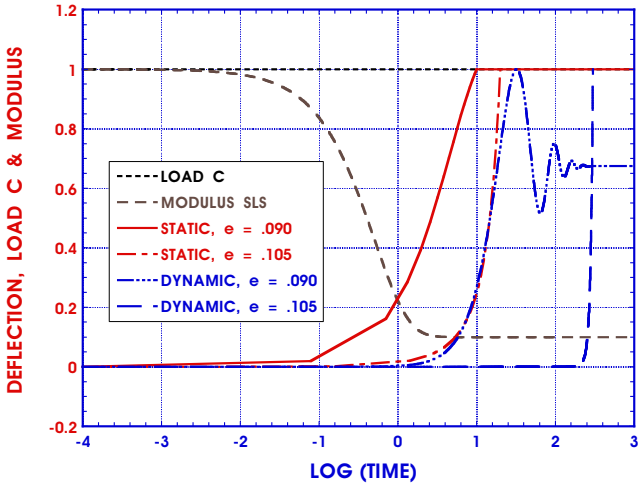

Figure 16: Quasi-static and dynamic deformations for $e = .090$ and .105, $\tau_1 = .5, \tau_2 = .05$, load C

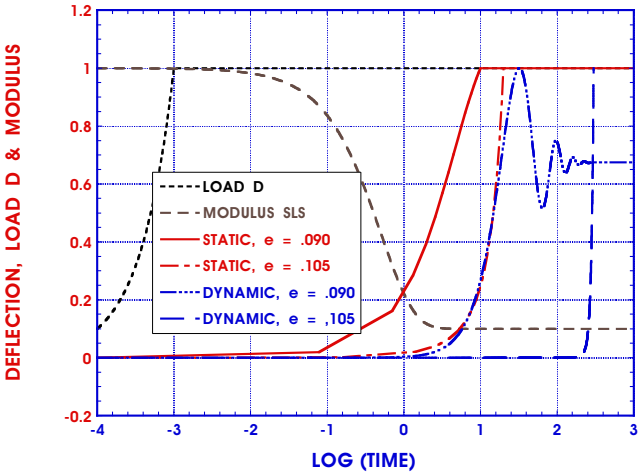

Figure 17: Quasi-static and dynamic deformations for $e = .090$ and .105, $\tau_1 = .5, \tau_2 = .05$, load D

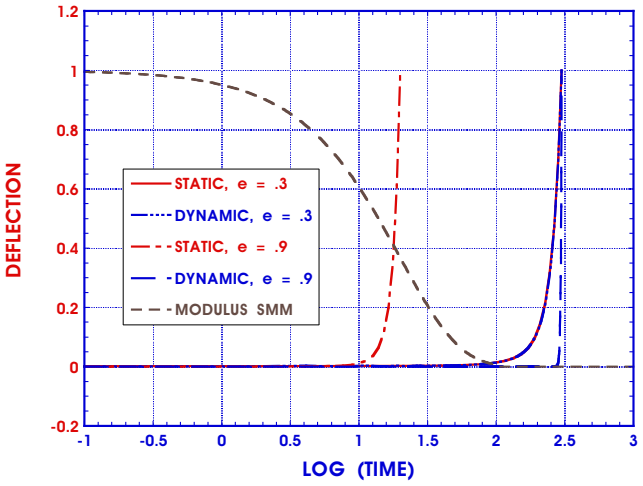

Figure 18: Quasi-static and dynamic SMM deformations for $e = .3$ and .9, $\tau = 20$, loads A - D

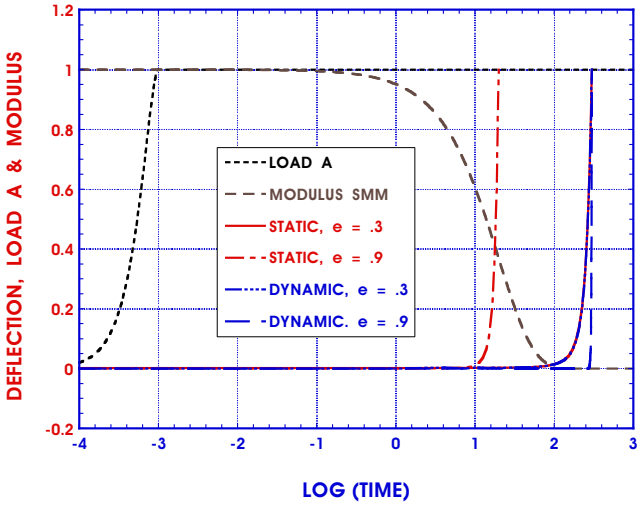

Figure 19: Quasi-static and dynamic SMM deformations for $e = .3$ and .9, $\tau = 20$, load A

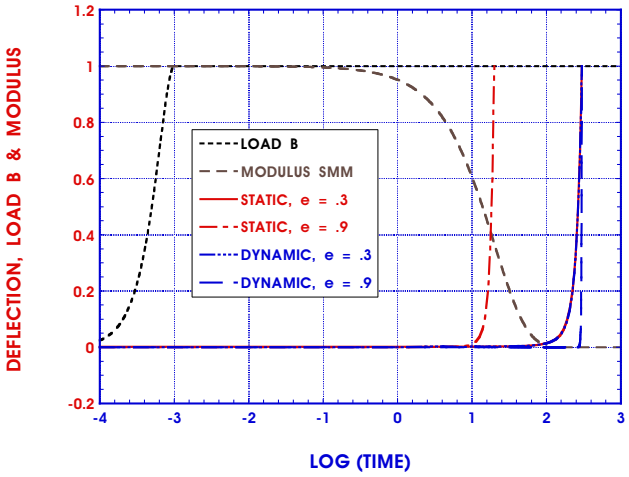

Figure 20: Quasi-static and dynamic SMM deformations for $e = .3$ and .9, $\tau = 20$, load B

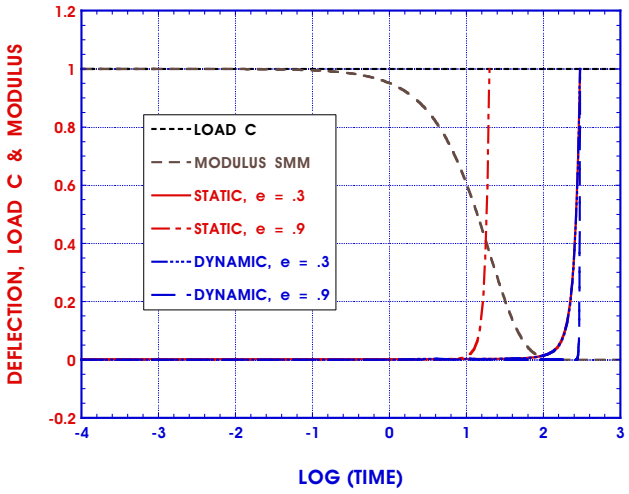

Figure 21: Quasi-static and dynamic SMM deformations for $e = .3$ and .9, $\tau = 20$, load C

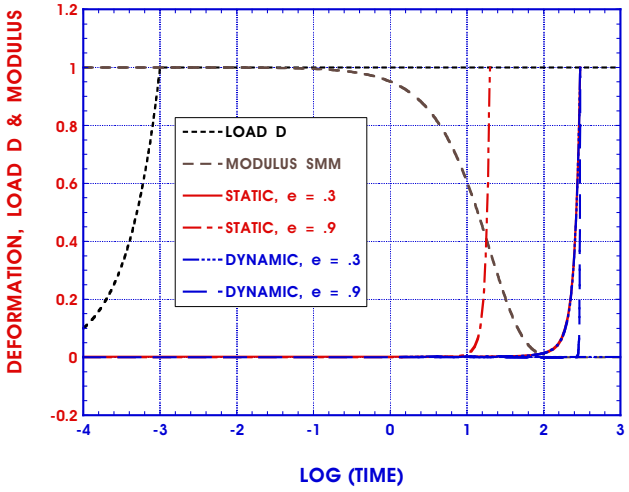

Figure 22: Quasi-static and dynamic SMM deformations for $e = .3$ and .9, $\tau = 20$, load D

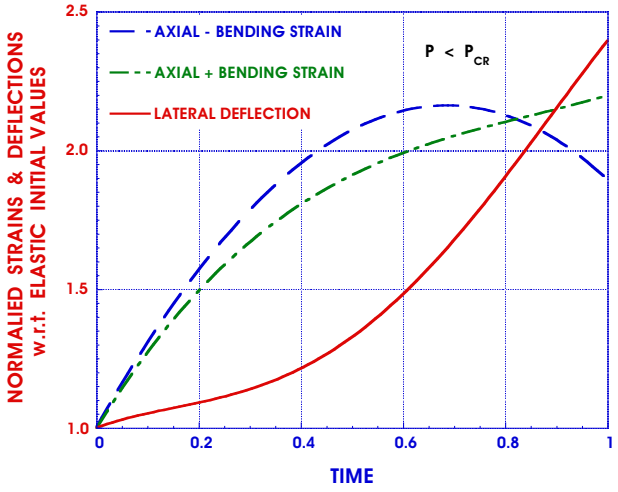

Figure 23: Viscoelastic column bending strain reversal

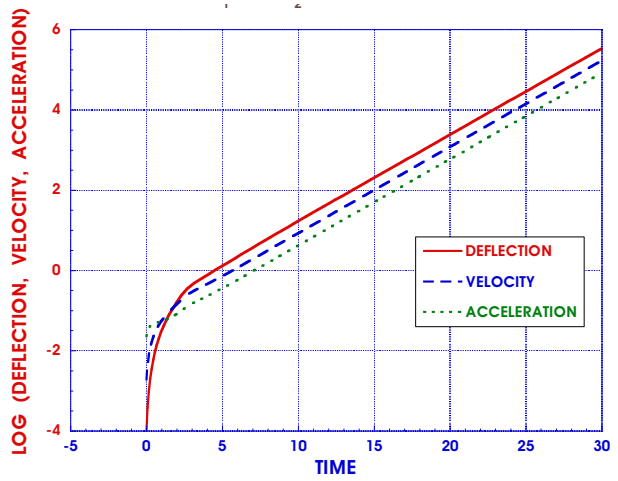

Figure 24: Dynamic kinematic variables for $e = .8, \tau_1 = .5, \tau_2 = .25$

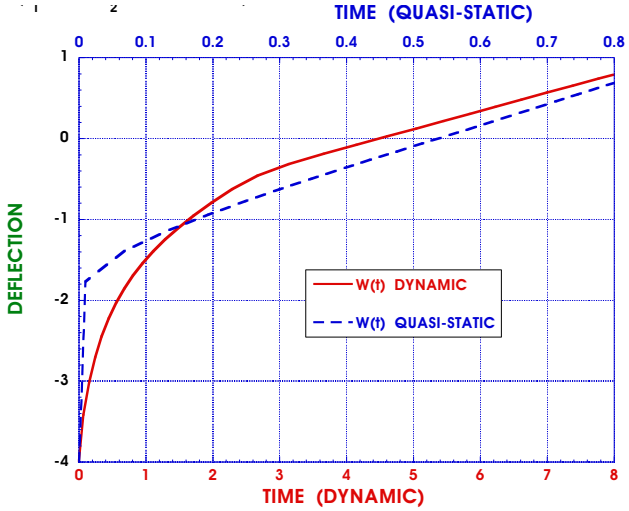

Figure 25: Quasi-static and dynamic SMM deformations for $e = .8, \tau_1 = .5, \tau_2 =, 25$, load A

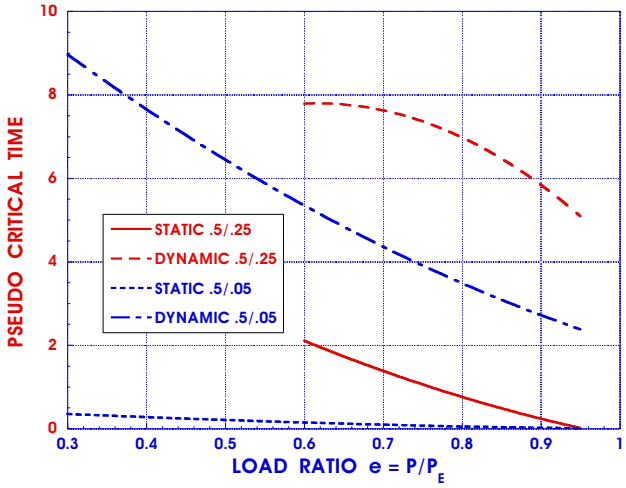

Figure 26: Pseudo critical time vs. load ratio

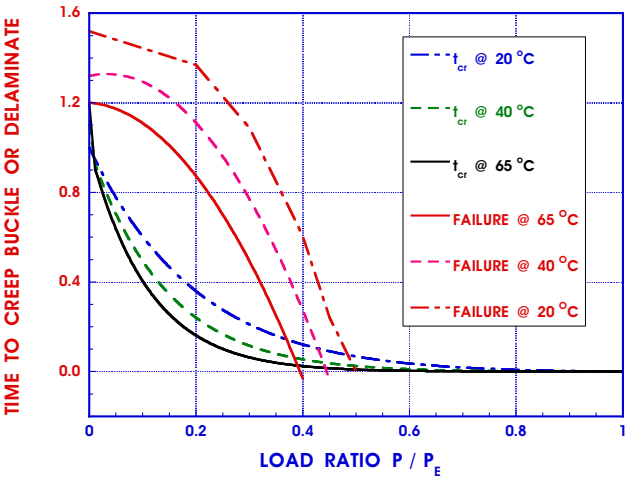

Figure 27: Creep buckling/torsional divergence and delamination onset times

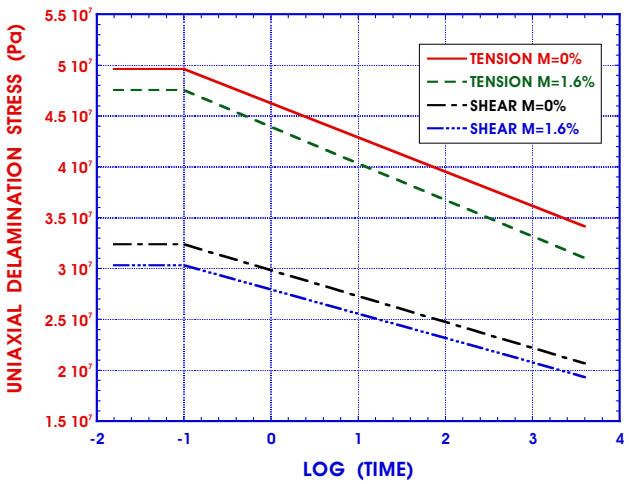

Figure 28: Uniaxial delamination creep strengths

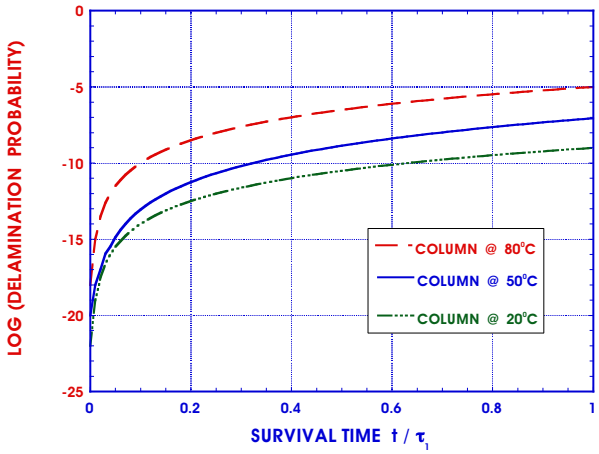

Figure 29: Probability of delamination onset vs. survival time

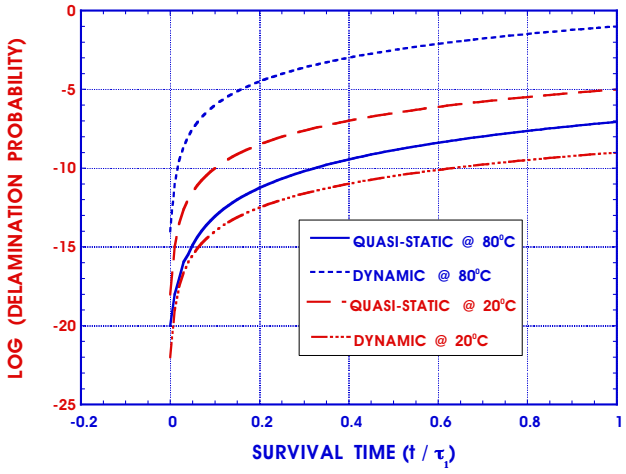

Figure 30: Probability of delamination onset for quasi-static and dynamic conditions